Advanced analytics for the SABR model*

A. Antonov and M. Spector
Numerix Quantitative Research†

March 23, 2012

Abstract

In this paper, we present advanced analytical formulas for SABR model option pricing. The first technical result consists of a new exact formula for the zero correlation case. This closed form is a simple 2D integration of elementary functions, particularly attractive for numerical implementation. The second result is an effective approximation of the general correlation case. We use a map to the zero correlation case having a nice behavior on strike edges. The map formulas are easily implemented and do not contain any numerical integration. These formulas are important in volatility surface construction and CMS product replication because they provide correct behavior for far strikes and reduced approximation error. The latter is also helpful for dynamic SABR models.

1 Introduction

The SABR model introduced in Hagan et al. (2002) is widely used by practitioners to capture skew and smile effects of interest rate swaptions. The underlying process F_t represents the Constant Elasticity of Variance (CEV) evolution with log-normal stochastic volatility v_t

$$dF_t = F_t^{\beta}\, v_t\, dW_1$$
$$dv_t = \gamma\, v_t\, dW_2$$

with some correlation $E[dW_1\, dW_2] = \rho dt$, power β, $0 < \beta < 1$, and absorbing boundary conditions.

The primary usage of the SABR model is volatility surface interpolation. For example, a swaption 1Y10Y with 1Y exercise and 10Y length has several quotes corresponding to different strikes. The SABR model attached to this swaption is calibrated in order to fit existing prices or implied volatilities. The calibrated model is used as an interpolation tool for other strikes.

*This is version 2 of the paper (July 23, 2011). Here we have updated the numerical experiment tables addressing MC convergence for small strikes and corrected a typo in the important formula (2.28) (we thank Abdelkader Ratnani for pointing it out). We have also added numerical experiments for the hybrid SABR ZC map. We have explicitly address the approximation procedure at the end of Section 2.2. Other changes are minor.

†Numerix LLC 150 East 42nd Street, 15th Floor, New York, NY 10017; antonov@numerix.com, mspector@numerix.com

Another important application of the SABR model consists of the calculation of European CMS products associated with the swap rate in hand. The CMS price is calculated via integrals of European swaption prices using a static replication formula (Hagan (2003)). The integration is done over swaption strikes from zero to infinity. This means that the SABR swaption pricer should be robust and coherent for all the strikes.

Finally, there is the SABR process application as a term structure model; see, for example, Rebonato et al. (2009) for the SABR/LIBOR Market Model or Mercurio and Morini (2009) for inflation models.

In the original article, Hagan et al. (2002) came up with an approximation formula for European option prices. The logic was based on a small time expansion which was refined later by many other authors, for example, Beresticky et al. (2004), Henry-Labordere (2008), Paulot (2009), Obloj (2008), and others. However, the approximation quality rapidly degrades with time, for example, for maturities larger than 10Y the error in implied volatility can be 1% or more even for ATM values. Moreover, one can easily observe bad approximation behavior for extreme strikes which sometimes prevents obtaining a valid probability density function. These undesired properties on the edges are especially dangerous for CMS calculations by static replication.

The initial Hagan et al. (2002) approximation formula is used as a standard tool for volatility surface interpolation, which has led somehow to the *approximation* rather than the *model* itself becoming an industry standard. However, the model price is more coherent and attractive.

A different approach to SABR option pricing was undertaken in Islah (2009) where the author contributed an exact formula in terms of a multi-dimensional integration for the zero correlation case and a conditional Bessel process approximation for non-zero correlation. Nevertheless, a practical implementation of Islah's exact result for calibration is hardly possible: The final formula consists of three-dimensional integration of special functions and appears to be slow numerically.

Finally, Andreasen and Huge (2011) proposed an approximation-based one-step PDE solver. The procedure was proven to be arbitrage-free (i.e., with valid probability density function), but still delivers an approximation for the SABR model.

In the present article[1], we improve the approximate results for SABR option pricing. Namely, our first technical contribution consists of an exact formula for the zero correlation case in terms of a simple 2D integration of elementary functions, or one-dimensional integral of a special function known as McKean kernel. The corresponding integrands have plausible asymptotics which permits an efficient numerical implementation suitable for tight time constraints for calibration.

The second technical result covers a general correlation case where we propose a very accurate approximation based on a model *map* procedure. Namely, we calculate effective coefficients of a zero correlation SABR model, the *map proxy*, such that its small time asymptotics coincide with the initial non-zero correlation case. Note that the efficient coefficient expressions involve simple algebra without numerical integration. Then, we calculate the option price using the effective zero correlation SABR model[2]; see Antonov-Misirpashaev (2009) for maps to other models.

Our new results provide strongly reduced approximation error and correct behavior on the edges of the distribution for most of model parameters. Note that for very rare situations (large correlations in absolute value and small power parameter) the option price can be occasionally non-convex for small strikes. However, this undesired effect is much less pronounced than that for previous approximations. Moreover,

[1] The results were first announced in Antonov-Spector (2011).

[2] Hagan at al. used the Black-Scholes model as the map proxy which has, of course, very different properties than the initial SABR model.

due to its small amplitude and localization it does not influence CMS pricing by static replication.

The high accuracy of our approximation is very important for dynamic SABR models where calibration procedures naturally require a close fit of analytics and real, for example, simulated result. Let us stress that, throughout the paper, we consider the *classical* SABR model with the stochastic volatility *without mean-reversion*. This property, however, does not seem to be very intuitive, especially for large time-horizons. Hopefully, our analytical results can be adapted to mean-reverting volatility setups.

The paper is organized as follows. In Section 2, we present the main results. In Section 3, we introduce the SABR Forward-Kolmogorov equation and discuss boundary conditions. Section 4 contains a derivation of the zero-correlation exact results while Sections 5 and 6 are devoted to the general correlation approximation. Finally, we provide numerical results in Section 7 and conclude in Section 8.

2 Main results

Consider the SABR process (Hagan et al. (2002)) for some rate F_t

$$dF_t = F_t^{\beta}\, v_t\, dW_1 \tag{2.1}$$

$$dv_t = \gamma\, v_t\, dW_2 \tag{2.2}$$

with some correlation $E[dW_1\, dW_2] = \rho$ and power β, $0 < \beta < 1$. The log-normal process v_t plays a role of stochastic volatility. Thus, we have the famous set of five parameters: $\{F_0, v_0, \beta, \gamma, \rho\}$. In general, the initial rate F_0 is fixed and the parameters $\{v_0, \beta, \gamma, \rho\}$ are used for calibration.

A natural choice of *boundary conditions* at the zero rate is an absorbing boundary which guarantees the martingale property of the rate. A probability of the rate being at zero is finite: The probability density function (PDF) has a delta-function located at zero.

Below we present advanced analytics for a call option price,

$$\mathcal{C}(T,K) = E[(F_T - K)^+] \tag{2.3}$$

or the option time-value

$$\mathcal{O}(T,K) = E[(F_T - K)^+] - (F_0 - K)^+. \tag{2.4}$$

It is useful to transform the SABR rate process F_t to a stochastic volatility Bessel process Q_t defined as

$$Q_t = \frac{F_t^{1-\beta}}{1-\beta}. \tag{2.5}$$

The process Q_t satisfies

$$dQ_t = \left(\nu + \frac{1}{2}\right)\, Q_t^{-1}\, v_t^2\, dt + v_t\, dW_1 \tag{2.6}$$

$$dv_t = \gamma\, v_t\, dW_2 \tag{2.7}$$

with the *Bessel index*

$$\nu = -\frac{1}{2(1-\beta)}. \tag{2.8}$$

2.1 Zero correlation case

In this subsection, we will present results of the zero correlation case. By a change of variables

$$V = \frac{v}{\gamma}, \quad V_0 = \frac{v_0}{\gamma}, \quad t \to \gamma^2 t \tag{2.9}$$

we can set $\gamma = 1$ to obtain the normalized form of the SABR evolution

$$dF_t = F_t^\beta \, V_t \, dW_1 \tag{2.10}$$

$$dV_t = V_t \, dW_2 \tag{2.11}$$

with zero correlation $E[dW_1 \, dW_2] = 0$.

An option price for zero correlation[3] can be presented in terms of a simple two-dimensional integral as

$$C(t,K,F_0) - (F_0 - K)^+ = \sqrt{K F_0} \frac{e^{-t/8}}{\sqrt{2\pi t}} \int_0^\infty \frac{dV}{V} \left(\frac{V}{V_0}\right)^{-1/2}$$

$$\left\{ \frac{1}{\pi} \int_0^\pi d\phi \frac{\sin\phi \ \sin(|\nu|\phi)}{b - \cos\phi} e^{-\frac{\xi_0(w)^2}{2t}} + \frac{\sin(|\nu|\pi)}{\pi} \int_0^\infty d\psi \frac{\sinh\psi}{b + \cosh\psi} e^{-|\nu|\psi} e^{-\frac{\xi_0(w)^2}{2t}} \right\} \tag{2.12}$$

where we have denoted coefficient

$$b = \frac{q_K^2 + q_0^2}{2 \, q_K \, q_0}$$

depending on the transformed values of the spot and strike

$$q_K = \frac{K^{1-\beta}}{1-\beta} \quad \text{and} \quad q_0 = \frac{F_0^{1-\beta}}{1-\beta}. \tag{2.13}$$

The function $\xi_0(w)$ in the exponent

$$\xi_0(w) = \operatorname{arcosh}\left\{ \frac{q_K^2 + q_0^2 + V^2 + V_0^2}{2VV_0} - \frac{q_K \, q_0}{VV_0} \cosh w \right\}$$

has an argument w defined differently for the two integrals

$$\begin{array}{lll} \cosh w = & \cos\phi & \text{for } \phi\text{-integral,} \\ \cosh w = & -\cosh\psi & \text{for } \psi\text{-integral.} \end{array}$$

The integration can be performed numerically in an efficient manner—the integrands are smooth functions of the parameters. Note that the above formula is exact.

We can further simplify the option price formula by introducing the heat kernel $G(t,s)$

$$G(t,s) = 2\sqrt{2} \frac{e^{-t/8}}{t\sqrt{2\pi t}} \int_s^\infty du \sqrt{\cosh u - \cosh s} \ \ u \, e^{-\frac{u^2}{2t}} \tag{2.14}$$

[3] We consider the general case below.

which is closely related to the McKean (1970) kernel $G_{MK}(t,s)$, namely $\frac{\partial G}{\sinh s \partial s} = -2\pi G_{MK}$. The result is given in the following compact form

$$C(t,K,F_0) - (F_0-K)^+ = \frac{2}{\pi}\sqrt{KF_0}\left\{\int_{s_-}^{s_+} ds \frac{\sin(|\nu|\phi(s))}{\sinh s} G(t,s) + \sin(|\nu|\pi)\int_{s_+}^{\infty} ds \frac{e^{-|\nu|\psi(s)}}{\sinh s} G(t,s)\right\} \tag{2.15}$$

with the following underlying functions

$$\phi(s) = 2\,\arctan\sqrt{\frac{\sinh^2 s - \sinh^2 s_-}{\sinh^2 s_+ - \sinh^2 s}} \tag{2.16}$$

$$\psi(s) = 2\,\mathrm{arctanh}\sqrt{\frac{\sinh^2 s - \sinh^2 s_+}{\sinh^2 s - \sinh^2 s_-}} \tag{2.17}$$

and the integration limits

$$s_- = \mathrm{arcsinh}\left(\frac{|q_K - q_0|}{V_0}\right) \tag{2.18}$$

$$s_+ = \mathrm{arcsinh}\left(\frac{q_K + q_0}{V_0}\right). \tag{2.19}$$

Note that the option price depends[4] on the parameters q_0, q_K and V_0 through dimensionless s_- and s_+.

Derivation details can be found in Section 4.

2.2 Non-zero correlation general case

In this subsection, we will announce results for an option price approximation for a general correlation. We will use mathematical results from the heat-kernel theory and will explain it in details later.

For a general correlation, we will use a small-time expansion giving the following formula for the option time-value

$$\mathcal{O}(T,K) = \frac{T^{\frac{3}{2}}}{2\sqrt{2\pi}}\,\exp\left\{-\frac{1}{2}\frac{s_{\min}^2}{T\gamma^2} - \ln\frac{s_{\min}^2}{2\gamma^2} + \ln\left(K^\beta\sqrt{v_0 v_{\min}}\right) - \mathcal{A}_{\min}\right\}. \tag{2.20}$$

Here optimal geodesic distance $s_{\min}$ is a function of the initial value of the rate, F_0, the initial stochastic volatility value v_0, and the strike K, defined as follows

$$s_{\min} = \left|\ln\frac{v_{\min} + \rho v_0 + \gamma\delta q}{(1+\rho)v_0}\right| \tag{2.21}$$

for

$$\delta q = \frac{K^{1-\beta} - F_0^{1-\beta}}{1-\beta} \tag{2.22}$$

and

$$v_{\min}^2 = \gamma^2\delta q^2 + 2\rho\gamma\delta q\, v_0 + v_0^2. \tag{2.23}$$

[4]Except the square root $\sqrt{KF_0}$

The function $\mathcal{A}_{\min}$ is the so-called optimal parallel transport

$$\mathcal{A}_{\min} = \frac{1}{2}\ln(K/F_0)^{\beta} + \mathcal{B}_{\min} \tag{2.24}$$

where contribution $\mathcal{B}_{\min}$ has a simple form

$$\mathcal{B}_{\min} = -\tfrac{1}{2}\frac{\beta}{1-\beta}\frac{\rho}{\sqrt{1-\rho^2}}\left(\pi - \varphi_0 - \arccos\rho - I\right) \tag{2.25}$$

with coefficients

$$L = \frac{v_{\min}}{q\,\gamma\,\sqrt{1-\rho^2}} \quad \text{and} \quad \varphi_0 = \arccos\left(-\frac{\delta q\,\gamma + v_0\,\rho}{v_{\min}}\right)$$

and integral

$$I = \begin{cases} \frac{2}{\sqrt{1-L^2}}\left(\arctan\frac{u_0+L}{\sqrt{1-L^2}} - \arctan\frac{L}{\sqrt{1-L^2}}\right) & \text{for } L<1 \\ \\ \frac{1}{\sqrt{L^2-1}}\ln\frac{u_0\left(L+\sqrt{L^2-1}\right)+1}{u_0\left(L-\sqrt{L^2-1}\right)+1} & \text{for } L>1 \end{cases} \tag{2.26}$$

where

$$q = \frac{K^{1-\beta}}{1-\beta}$$

and

$$u_0 = \frac{\delta q\,\gamma\rho + v_0 - v_{\min}}{\delta q\,\gamma\sqrt{1-\rho^2}}.$$

See also Henry-Labordere (2008) and Paulot (2009).

The small time expansion works fine for small times, but for moderate and large ones ones it needs to be imroved. We can use the mapping technique (see Antonov-Misirpashaev (2009)) which works as follows. We come up with another model having the same small time expansion for the option (mimicking model) and calculate the final result using the mimicking model. For example, Hagan used the Black-Scholes model or normal one for this. Paulot has proposed the CEV model as the mimicking model. We will go further and use the SABR model with zero correlation (SABR ZC) having similar characteristics and asymptotics to the initial SABR model.

Denote the SABR ZC parameters with tilde and set its skew and vol-of-vol in a strike-independent manner

$$\tilde{\beta} = \beta \tag{2.27}$$

$$\tilde{\gamma}^2 = \gamma^2 - \frac{3}{2}\left\{\gamma^2\rho^2 + v_0\gamma\rho\,(1-\beta)\,F_0^{\beta-1}\right\} \tag{2.28}$$

and define as usual

$$\delta\tilde{q} = \frac{K^{1-\tilde{\beta}} - F_0^{1-\tilde{\beta}}}{1-\tilde{\beta}}. \tag{2.29}$$

The initial stochastic volatility value $\tilde{v}_0$ can be calculated as expansion

$$\tilde{v}_0 = \tilde{v}_0^{(0)} + T\,\tilde{v}_0^{(1)} + \cdots \tag{2.30}$$

The leading term can be expressed as

$$\tilde{v}_0^{(0)} = \frac{2\,\Phi\,\delta\tilde{q}\,\tilde{\gamma}}{\Phi^2 - 1} \tag{2.31}$$

where

$$\Phi = \left(\frac{v_{\min} + \rho v_0 + \gamma\,\delta q}{(1+\rho)v_0}\right)^{\frac{\tilde{\gamma}}{\gamma}}.$$

The (first) correction to the initial stochastic volatility of the mimicking model can be expressed in an algebraic form of the initial model parameters, the strike, and the leading order value $\tilde{v}_0^{(0)}$

$$\frac{\tilde{v}_0^{(1)}}{\tilde{v}_0^{(0)}} = \tilde{\gamma}^2\,\frac{\frac{1}{2}\,(\beta-\tilde{\beta})\ln(K\,F_0) + \frac{1}{2}\ln\left(v_0 v_{\min}\right) - \frac{1}{2}\ln\left(\tilde{v}_0^{(0)}\,\sqrt{\delta\tilde{q}^2\,\tilde{\gamma}^2 + \tilde{v}_0^{(0)\,2}}\right) - \mathcal{B}_{\min}}{\frac{\Phi^2-1}{\Phi^2+1}\ln\Phi}. \tag{2.32}$$

Thus, given option strike K, the coefficients of the initial SABR model, and the postulated free SABR ZC parameters (2.27-2.28), we calculate the effective initial value value of the stochastic volatility as the first order expansion (2.30) with the leading term (2.31) and its correction (2.32). This defines all parameters of the mimicking SABR ZC model. A call option price for the strike K is thus approximated by the constructed mimicking model—a zero correlation SABR model—for which the analytical option price is available and given by (2.12).

The ATM case is a cumbersome but straightforward limit $K \to F_0$. The leading order ATM value reads[5]

$$\tilde{v}_0^{(0)}\Big|_{K=F_0} = v_0. \tag{2.33}$$

The first ATM correction can be also expressed in simple terms

$$\left.\frac{\tilde{v}_0^{(1)}}{\tilde{v}_0^{(0)}}\right|_{K=F_0} = \frac{1}{12}\,\left(1 - \frac{\tilde{\gamma}^2}{\gamma^2} - \frac{3}{2}\rho^2\right)\gamma^2 + \frac{1}{4}\,\beta\,\rho\;\; v_0\gamma\,F_0^{\beta-1}. \tag{2.34}$$

Note that its last term comes from the second derivative of the integral $\mathcal{B}$. It can be also found in the formula of Hagan et al. (2002).

We can construct a "hybrid" solution for effective volatilities. Namely, for a *general*, not necessarily ATM strike, use the optimal strike-dependent leading order initial volatility (2.31) and the *ATM correction* (2.34). We address property of this simple solution in the Section 7.

The general case $\beta \neq \tilde{\beta}$ is slightly more complicated resulting in the following leading order effective volatility

$$\tilde{v}_0^{(0)}\Big|_{K=F_0} = v_0\,F_0^{\beta-\tilde{\beta}} \tag{2.35}$$

and its correction

$$\left.\frac{\tilde{v}_0^{(1)}}{\tilde{v}_0^{(0)}}\right|_{K=F_0} = \frac{1}{12}\,\left(1 - \frac{\tilde{\gamma}^2}{\gamma^2} - \frac{3}{2}\rho^2\right)\gamma^2 + \frac{1}{4}\,\beta\,\rho\;\; v_0\gamma\,F_0^{\beta-1} + \frac{1}{24}\,v_0^2 F_0^{2\beta-2}\left((\beta-1)^2 - (\tilde{\beta}-1)^2\right). \tag{2.36}$$

[5]Here, we explicitly set $\tilde{\beta} = \beta$ as prescribed by (2.27).

Finally, we summarize the approximation procedure. Given the SABR model with non-zero correlation (2.1-2.2), strike K and maturity T, we come up with (strike dependent) mimicking process $\tilde{F}_t$ and $\tilde{v}_t$

$$d\tilde{F}_t = \tilde{F}_t^{\tilde{\beta}}\,\tilde{v}_t\,d\tilde{W}_1 \tag{2.37}$$

$$d\tilde{v}_t = \tilde{\gamma}\,\tilde{v}_t\,d\tilde{W}_2 \tag{2.38}$$

with zero correlation between the driving Brownian motions $\mathbb{E}[d\tilde{W}_1\,d\tilde{W}_2] = 0$. The efficient parameters are calculated as follows: the skew $\tilde{\beta} = \beta$, the vol-of-vol $\tilde{\gamma}$ as (2.28) and the initial (strike dependent) effective volatility $\tilde{v}_0 = \tilde{v}_0^{(0)} + T\,\tilde{v}_0^{(1)}$ as (2.31-2.32). The approximate call option price

$$\mathcal{C}(T,K) \simeq \mathbb{E}[(\tilde{F}_T - K)^+]$$

is finally computed by the numerical integration (2.15) or other equivalent formula.

2.3 Asymptotics

In this section, we consider the vol-of-vol γ as not being unity and operate with process v_t (2.7) instead of V_t (2.11) and corresponding stretched time $t\gamma^2$.

Being equipped with an exact solution for the zero correlation case, we can obtain asymptotics for small and large strikes. Below we present the results in terms of the Bessel form of the SABR process (2.6) where we have replaced the SABR process F_t by $Q_t = \frac{F_t^{1-\beta}}{1-\beta}$. Obviously, the initial SABR density function $P(t,F) = E[\delta(F_t - F)]$ can be related with the Bessel process PDF $P(t,q) = E[\delta(Q_t - q)]$ by $dFP(t,F) = dqP(t,q)$.

At the end of section 4.1, we have derived small strike behavior, which we present here for $\gamma \neq 1$

$$p\,(t,q\mid q_0) = 4q\,\frac{(|\nu|+1)\,v_0^2(\gamma\,q_0)^{2|\nu|+2}e^{-t\gamma^2/8}}{-2\pi i\sqrt{2\pi t\gamma^2}}\int_0^\infty \frac{dv}{v_0}\left(\frac{v_0}{v}\right)^{1/2}\int_{-\infty}^{\infty}\frac{d\xi\,\sinh\xi\,e^{-\frac{(\xi+i\pi)^2}{2t\gamma^2}}}{(\gamma^2\,q_0^2+v^2+v_0^2+2vv_0\cosh\xi)^{|\nu|+2}}.$$

The asymptotic is linear in q. However, we did not manage to simplify the coefficient which is, of course, positive and real in spite of a presence of the imaginary unit.

Section 4.3 gives a leading order of large strike asymptotics

$$p(t,q) \sim e^{-\frac{1}{2t\gamma^2}\,\ln^2\frac{2q\,\gamma}{v_0}} \tag{2.39}$$

which coincides with that given by the heat-kernel small time expansion (2.20) where the geodesic distance $s_{\min} \sim \ln(\frac{2\,q\,\gamma}{v_0})$. One can also "quantify" the notion of the *large* q and the strike

$$q \sim \frac{v_0}{\gamma}e^{3\gamma\sqrt{t}} \tag{2.40}$$

or, in terms of the strikes

$$K \sim \left(\frac{(1-\beta)\,v_0}{\gamma}\right)^{\frac{1}{1-\beta}}\,e^{\frac{3\gamma\sqrt{t}}{1-\beta}}. \tag{2.41}$$

See Section 4.3 for details. A log-volatility of a rate is of order of 20%, thus $v_0 \sim 0.2\,F_0^{1-\beta}$. The vol-of-vol can have also the same order of $20\% - 40\%$. Thus, a large strike is approximately

$$K \sim F_0\,(1-\beta)^{\frac{1}{1-\beta}}\,e^{\frac{\sqrt{t}}{1-\beta}}. \tag{2.42}$$

Accordingly, for small β (corresponding to the "normal" case) the distribution is quite narrow even for moderate maturities. On the other hand, a log-normal case $\beta \to 1$ gives very fat wings and a "large strike" can exceed the initial rate value by multiple orders.

For the general correlation case, one can show that the PDF will retain linear asymptotics in q for small strikes

$$p(t,q) \sim q. \tag{2.43}$$

See Section 3. For large strikes, the leading asymptotics correspond to its small-time counterpart obtained by the heat-kernel small time-expansion

$$p(t,q) \sim e^{-\frac{1}{2t\gamma^2}\,\ln^2\frac{2q\,\gamma}{(1+\rho)v_0}}. \tag{2.44}$$

This is an intuitive result without a strict proof, however.

The approximation gives a close fit for the distribution for a wide range of strikes. However, very rarely, the approximate PDF can have small negative values for small strikes (for small β and large ρ). Of course, these negative values are tiny w.r.t. huge negative probabilities for existing approximationa based on the effective implied volatility. For large strikes, our approximation numerically appears to be close to the heat-kernel small time expansion (2.44); we will address it rigorously elsewhere.

3 SABR density PDE: absorbing and reflecting solutions

In this section, we study the SABR density general properties. Starting with the SDE for the Bessel process with stochastic volatility (BES SV) (2.6), we address boundary conditions in terms of the PDF behavior at zero, identify them with absorbtion and reflection, and comment on the norm and moment conservation.

The BES SV process gives rise to the Forward Kolmogorov equation

$$p_t = -\left(\nu+\frac{1}{2}\right)\,v^2\,\left(q^{-1}\,p\right)_q + \frac{1}{2}\,v^2 p_{qq} + \rho\gamma\left(v^2\,p\right)_{qv} + \frac{1}{2}\gamma^2\left(v^2\,p\right)_{vv} \tag{3.1}$$

which delivers a solution for the density $p(t,q,v) = E[\delta(q_t-q)\,\delta(v_t-v)]$ with the initial condition $p(0,q,v) = \delta(q_0-q)\,\delta(v_0-v)$. The solution is unique provided that certain boundary conditions are imposed at $q=0$.

As in the pure Bessel case, see, for example, Jeanblanc et al. (2009), we look for a solution at small q in the form

$$p(t,q,v) = q^{\kappa}\,\phi(t,q,v)$$

where function $\phi(t,q,f)$ is regular at $q=0$. A balance of leading terms (of the order of $q^{\kappa-2}$) determines two possible characteristic exponents, $\kappa_1 = 1$ and $\kappa_2 = 2\nu+1$, and thus gives rise to the following solutions

$$p^{(1)} = q\left(C_0 + C_1 q + O(q^2)\right), \tag{3.2}$$

$$p^{(2)} = q^{2\nu+1}\left(B_0 + B_1 q + O(q^2)\right). \tag{3.3}$$

Note that the second one may be realized only for $\nu > -1$ as follows from the integrability condition, $2\nu+1 > -1$. Considering the next order leads to

$$\begin{aligned} v^2 C_1 &= -\frac{2\rho}{1-2\nu}\left(v^2 C_0\right)_v \\ v^2 B_1 &= -2\rho\left(v^2 B_0\right)_v. \end{aligned} \tag{3.4}$$

For the zero correlation the first order coefficients cancel out.

Let us examine these asymptotics of being absorbing or reflecting. We notice that the marginal distribution of the stochastic volatility v_t is log-normal

$$p(t,v) = \int dq\, p(t,q,v) = \frac{1}{\sqrt{2\pi t\gamma^2}}\; v^{-1}\; e^{-\frac{1}{2}\frac{\left(\ln v + \frac{1}{2}t\gamma^2\right)^2}{t\gamma^2}}. \tag{3.5}$$

This means that for any fixed q the PDF $p(t,q,v)$ goes to zero for $v \to 0$ with all its derivatives over v. This property permits us to understand the asymptotic behavior of the marginal distribution of q_t

$$p(t,q) = \int dv\, p(t,q,v). \tag{3.6}$$

Indeed, integrating the Forward Kolmogorov equation over v, we obtain[6]

$$\partial_t\, p(t,q) = \int dv\, v^2 \left(-\left(\nu + \frac{1}{2}\right) \left(q^{-1}\, p\right)_q + \frac{1}{2} p_{qq} \right). \tag{3.7}$$

A time dependence of the norm

$$n(t) = \int dq\, dv\, p(t,q,v)$$

is established by the integration of the equation (3.7) over q and occurs to be dependent on the PDF behavior at the $q = 0$ boundary,

$$\partial_t\, n(t) = \int dv\, v^2 \left(\left(\nu + \frac{1}{2}\right)\, q^{-1}\, p - \frac{1}{2}\, p_q \right)_{q\to 0}. \tag{3.8}$$

For the solution (3.2), we get

$$\partial_t\, n^{(1)}(t) = \nu \int dv\, v^2 C_0(t,v)$$

while for the solution (3.3) the factor to be integrated becomes

$$\left(\left(\nu + \frac{1}{2}\right)\, q^{-1}\, p - \frac{1}{2}\, p_q \right)_{q\to 0} = -\frac{1}{2} q^{2\nu+1} \left(B_1 + O(q)\right)$$

and does not necessarily turn into zero at $q \to 0$. Indeed, we have $-1 < 2\nu + 1 < 0$ in the interval $0 < \beta < \frac{1}{2}$. However, integrating over v cancels the potentially singular term due to (3.4)

$$\int dv\, v^2 B_1(t,v) = -2\rho \int dv\, \left(v^2 B_0\right)_v = 0$$

and results in the norm conservation

$$\partial_t\, n^{(2)}(t) = 0.$$

Thus, the norm-conserving solution $p^{(2)}$ (3.3) is naturally identified as reflecting, and the solution $p^{(1)}$ (3.2) which reveals the norm defect (at negative ν) is identified as absorbing.

[6] We used the boundary properties of the density for $v \to 0$ to zero the two last terms.

Though interested mainly in negative index ν ($\beta < 1$), we comment briefly on the case $\nu > 0$. Imagine that the total PDF is presented by some combination of the solutions $p^{(1)}$ and $p^{(2)}$. For small q, the leading term of $p^{(1)} \sim q$ dominates the leading term of $p^{(2)} \sim q^{2\nu+1}$ implying that

$$p = p^{(1)} + p^{(2)} \simeq C_0(t,v)q$$
$$\partial_t\, n(t) = \partial_t\, n^{(1)}(t) + \partial_t\, n^{(2)}(t) = \nu \int dv\, v^2 C_0(t,v).$$

These relations, however, are in conflict. On the one hand, C_0 must be positive to define positive PDF p. Both ν and C_0 being positive, the time derivative of the norm must also be positive, $\partial_t\, n(t) > 0$, which is probabilistically impossible. Indeed, if the initial distribution is normalized to one, $n(0) = 1$, the norm $n(t)$ has no room to grow farther. Thus, the absorbing solution $p^{(1)}$ may be realized only at $\nu < 0$ ($\beta < 1$). In this case, the norm defect, $\partial_t\, n(t) < 0$, merely indicates that there is a finite probability for process q_t to be at zero which is natural for the absorbing solution, $P(q_t = 0) = 1 - n(t)$.

We conclude that for a positive index $\nu > 0$ ($\beta > 1$) there exists only reflecting solution $p^{(2)}$ while for $\nu < -1$ ($\frac{1}{2} < \beta < 1$) the only possible solution is the absorbing one $p^{(1)}$. In these intervals of the index ν the PDF p is completely determined by the inner dynamics of the random processes q_t and v_t with no freedom for an outside boundary condition at $q = 0$. In the interval $-1 < \nu < 0$ ($\beta < \frac{1}{2}$) both solutions are legitimate, and we have to impose a boundary condition at $q = 0$ to select the proper unique solution. As we have seen, a selection of the reflecting solution is associated with the requirement of the norm conservation. Below we prove that a selection of the absorbing solution (and ignoring the reflecting one) is related with the martingale property of the SABR process F_t. Indeed, in terms of the BES SV process we need to calculate the (-2ν)-th moment $m_{-2\nu}(t)$ as far as the rate process reads $F_t = q_t^{-2\nu}\,(-2\nu)^{2\nu}$.

Multiplying the Forward Kolmogorov equation (3.1) by $q^{-2\nu}$ and rearranging terms we obtain

$$q^{-2\nu}\, p_t = \frac{1}{2}\, v^2\, \left(q^{-2\nu+1}\,(p\, q^{-1})_q\right)_q + \left[\rho\gamma\, q^{-2\nu}\, \left(v^2\, p\right)_q + \frac{1}{2}\gamma^2\, q^{-2\nu}\, \left(v^2\, p\right)_v\right]_v . \tag{3.9}$$

Thus, the moment time-derivative

$$\partial_t\, m_{-2\nu}(t) = \int dq\, dv\, q^{-2\nu}\, p_t(t,q,v) = -\frac{1}{2}\int dv\, v^2\, \left(q^{-2\nu+1}\,(p\, q^{-1})_q\right)_{q=0} \tag{3.10}$$

has the following form for each of the solutions $p^{(1)}$ and $p^{(2)}$

$$\partial_t\, m^{(1)}_{-2\nu}(t) = 0$$
$$\partial_t\, m^{(2)}_{-2\nu}(t) = -\nu \int dv\, v^2\, B_0(t,v).$$

This indicates that the SABR process is a global martingale for the absorbing solution and a strict local one for the reflecting solution.

Below we will consider the SABR model with *absorbing boundary* as the most coherent and standard one.

4 Zero-correlation formulas

This section is devoted to the derivation of the option price formula for the zero correlation SABR model. Here, for simplicity, we consider the vol-of-vol γ equal to one using the transform (2.9).

Before starting our analysis, transform (2.5) the rate process F_t into the Bessel process Q_t, which satisfies

$$dQ_t = \left(\nu + \frac{1}{2}\right) Q_t^{-1} V_t^2 \, dt + V_t \, dW_1 \tag{4.1}$$

$$dV_t = V_t \, dW_2. \tag{4.2}$$

The zero correlation permits "absorbing" the stochastic volatility V_t into the new stochastic time τ

$$\tau_t = \int_0^t V_{t'}^2 dt'. \tag{4.3}$$

Indeed, the new process

$$dB_{1\tau} = V_t dW_{1t}$$

is a Brownian motion in time τ

$$\langle (dB_{1\tau})^2 \rangle = V_t^2 \langle (dW_{1t})^2 \rangle = V_t^2 dt = d\tau.$$

Process $B_{1\tau}$ also remains uncorrelated with W_2. Denote the process Q_t measured in the new time τ by $R_\tau \equiv Q_t$. Its governing SDE looks like

$$dR = (\nu + \tfrac{1}{2}) \frac{d\tau}{R} + dB_{1\tau}.$$

In other words, the process R_τ is a Bessel process with index ν.

4.1 The marginal PDF

In this subsection, we address the marginal distribution of the BES SV process Q_t defined as

$$p\left(t, q \mid q_0, V_0\right) = \mathbb{E}_{\{W_2\}} \mathbb{E}_{\{W_1\}} \left\{\delta(Q_t - q) | q_0, V_0\right\} = \mathbb{E}_{\{W_{2t}\}} \left\{ \left[\mathbb{E}_{\{B_{1\tau}\}} \left\{\delta(R_\tau - q) | q_0\right\} \right] | V_0 \right\}. \tag{4.4}$$

We concentrate on the PDF for $q > 0$ because the call option price does not depend on the (finite) probability of $Q_t = 0$.[7]

Since $B_{1\tau}$ remains uncorrelated with W_{2t}, the inner average is the single point PDF of Bessel process $BES^{(\nu)}$ with negative index ν and absorbing boundary condition (see, for example, Jeanblanc et al. (2009))

$$p^{(\nu)}(\tau, q | q_0) = 2q \frac{e^{-\frac{q^2+q_0^2}{2\tau}}}{2\tau} \left(\frac{q}{q_0}\right)^\nu I_{-\nu}\left(\frac{q q_0}{\tau}\right) \tag{4.5}$$

for $q > 0$.

The marginal PDF can be expressed in terms of the stochastic time τ_t density $p(t, \tau) = \mathbb{E}[\delta(\tau_t - \tau)]$

$$p\left(t, q \mid q_0, V_0\right) = \mathbb{E}_{\{W_{2t}\}} \left\{ p_{BES}^{(\nu)}(\tau_t, q | q_0) \right\} = \int_0^\infty d\tau \; p_{BES}^{(\nu)}(\tau, q \mid q_0) \; p(t, \tau). \tag{4.6}$$

[7] The finite probability $\mathbb{P}[Q_t = 0]$ for our absorbing boundary condition can be computed requiring the unit norm, i.e. $\mathbb{P}[Q_t = 0] = 1 - \int_{+0}^{\infty} dq \, p\left(t, q \mid q_0, V_0\right)$.

One can calculate the density $p(t,\tau)$ from the joint distribution function of τ_t and V_t, $p\,(t,\tau,V \mid V_0) = \mathbb{E}\left[\delta(\tau_t-\tau)\;\delta(V_t-V)\right]$, obtained by Yor (1992). Thus, to calculate the marginal PDF $p\,(t,q \mid q_0)$ we can proceed as follows

$$p\,(t,q \mid q_0) = \int d\tau\; p^{(\nu)}(\tau,q \mid q_0) \int dV\; p\,(t,\tau,V \mid V_0)\,.$$

We recall here the Yor result[8]

$$p(t,V^2,\tau\;|V_0^2) = \frac{e^{-t/8}}{V^2}\left(\frac{V^2}{V_0^2}\right)^{-1/4}\;\frac{e^{-\frac{V^2+V_0^2}{2\tau}}}{2\tau}\vartheta\left(\frac{V\,V_0}{\tau},t\right) \tag{4.7}$$

where function $\vartheta(r,t)$ is defined as

$$\vartheta(r,t) = \frac{re^{\frac{\pi^2}{2t}}}{\pi\sqrt{2\pi t}}\int_0^{+\infty} e^{-r\cosh\xi-\frac{\xi^2}{2t}}\;\sinh\xi\sin\frac{\pi\xi}{t}d\xi \tag{4.8}$$

$$= \frac{r}{(-2\pi i)\sqrt{2\pi t}}\int_{-\infty}^{+\infty} e^{-r\cosh\xi-\frac{(\xi+i\pi)^2}{2t}}\;\sinh\xi\;d\xi. \tag{4.9}$$

Despite looking different, two last expressions are equal, as readily seen by developing the exponent $\exp\left(-\frac{(\xi+i\pi)^2}{2t}\right)$ and keeping only the even part of the integrand in (4.9). The more compact form (4.9) may be preferable when making various transforms and trying to use analytical properties of functions after moving into complex plane ξ.

In Appendix A, we describe a simple derivation of the joint PDF of V_t^2 and τ_t based on arguments close to Yor's. The key elements include the Laplace transform (LT) in time which represents, in essence, passing to a random exponential time. Then, we make use of the Lamperti property of a geometric Brownian motion, which states that a geometrical Brownian motion

$$X_t^{(\nu)} = \exp(2\nu t + 2W_t)$$

measured in the stochastic time $\tau_t = \int_0^t X_{t'}dt'$, becomes a Squared Bessel process $X_t^{(\nu)} \equiv \rho_{\tau_t}^{(\nu)}$ with index ν (not to be confused with ν used earlier for process Q_t). Next, we apply the Girshanov theorem which allows us by change of measure to eliminate "path-dependent" factors. As a result, the LT of the joint PDF (4.7) proves to be proportional to the distribution of a Bessel process $\rho_\tau^{(\mu)}$ with index $\mu = (\nu^2+2\lambda)^{1/2}$ depending on the Laplace parameter λ and the original index ν. Finally, the inverse Laplace transform leads to the expressions (4.7-4.8).

Thus, we come up with the following expression for the joint PDF of Q_t and V_t

$$p\,(t,q,V \mid q_0,V_0) = 2V\frac{e^{-t/8}}{V^2}\left(\frac{V}{V_0}\right)^{-1/2}\int_0^\infty d\tau\; p^{(\nu)}(\tau,q|q_0)\frac{e^{-\frac{V^2+V_0^2}{2\tau}}}{2\tau}\vartheta\left(\frac{VV_0}{\tau},t\right). \tag{4.10}$$

Note inter alia that it is possible to present the LT of the joint density of Q_t and V_t in a compact and nice convolution form

$$\hat{p}\,(\lambda,q,V \mid q_0,V_0) = \frac{1}{V^2}\left(\frac{V}{V_0}\right)^{-(\mu+1/2)}\;\int_0^\infty d\tau\; p_{BES}^{(\nu)}(\tau,q|q_0)\;p_{BES}^{(\mu)}(\tau,V|V_0) \tag{4.11}$$

[8]We have denoted the PDF of the stochastic time τ and the *square* V_t^2 as $p(t,V^2,\tau\;|V_0^2) = \mathbb{E}\left[\delta(V_t^2-V^2)\,\delta(\tau_t-\tau)\right]$. Obviously, $p(t,\tau,V \mid V_0) = 2V\;p(t,V^2,\tau\;|V_0^2)$.

for $\mu = (\frac{1}{4} + 2\lambda)^{1/2}$. To our knowledge, this formula is new but we will not use it in our option price derivation.

Integrating the joint density (4.10) over volatility V, we obtain a marginal distribution of Q_t

$$p\left(t, q \mid q_0\right) = e^{-t/8} \int_0^\infty \frac{2dV}{V} \left(\frac{V}{V_0}\right)^{-1/2} \int_0^\infty d\tau \; p^{(\nu)}(\tau, q|q_0) \; \frac{e^{-\frac{V^2+V_0^2}{2\tau}}}{2\tau} \vartheta\left(\frac{VV_0}{\tau}, t\right). \tag{4.12}$$

At the end of this subsection, we address the small q (or small F) expansion. Indeed, we obtain the leading term of $p^{(\nu)}(\tau, q|q_0)$ for $q \to 0$, the PDF of the Bessel process (4.5), taking into account the small argument asymptotics of the Bessel function $I_{-\nu}(x)$

$$p^{(\nu)}(\tau, q|q_0) \simeq \frac{1}{\Gamma(|\nu|+1)} \frac{q}{\tau} \left(\frac{q_0^2}{2\tau}\right)^{|\nu|} e^{-\frac{q_0^2}{2\tau}}.$$

Then, substitute it into the formula (4.12)

$$p\left(t, q \mid q_0\right) \simeq \frac{2q}{\Gamma(|\nu|+1)} e^{-t/8} \int_0^\infty \frac{2dV}{V} \left(\frac{V}{V_0}\right)^{-1/2} \int_0^\infty \frac{d\tau}{(2\tau)^2} \left(\frac{q_0^2}{2\tau}\right)^{|\nu|} e^{-\frac{q_0^2+V^2+V_0^2}{2\tau}} \vartheta\left(\frac{VV_0}{\tau}, t\right).$$

Next, using expression (4.9) for the function ϑ, we can integrate over τ

$$\int_0^\infty \frac{d\tau}{\tau} \left(\frac{1}{2\tau}\right)^{|\nu|+2} e^{-\frac{A}{2\tau}} = \frac{\Gamma(|\nu|+2)}{A^{|\nu|+2}}$$

resulting in a linear asymptotic in q

$$\begin{aligned} p\left(t, q \mid q_0\right) \simeq 4q(|\nu|+1) \frac{V_0^2}{q_0^2} \int_0^\infty \frac{dV}{V_0} \left(\frac{V}{V_0}\right)^{-1/2} \\ \int_{-\infty}^\infty \frac{d\xi \; \sinh\xi}{-2\pi i} \left(\frac{q_0^2}{q_0^2 + V^2 + V_0^2 + 2VV_0\cosh\xi}\right)^{|\nu|+2} \frac{e^{-\frac{(\xi+i\pi)^2}{2t} - t/8}}{\sqrt{2\pi t}}, \end{aligned}$$

confirming our general result derived for any correlation. Unfortunately, the integral coefficient can hardly be simplified.

4.2 Option pricing

Integrating the marginal q distribution with a given payoff generates the option price in the form

$$C_{sabr}(t, K, F_0) = e^{-t/8} \int_0^\infty \frac{2dV}{V} \left(\frac{V}{V_0}\right)^{-1/2} \int_0^\infty d\tau \; C_{cev}(\tau, K, F_0) \frac{e^{-\frac{V^2+V_0^2}{2\tau}}}{2\tau} \vartheta\left(\frac{VV_0}{\tau}, t\right) \tag{4.13}$$

where $C_{cev}(\tau, K, F_0)$ is the τ-time value of the corresponding option in the CEV model.

An analogous formula served as a basis for the approach used by Islah (2009). CEV option values were expressed through χ^2 probability distributions, each presented as the integral of the corresponding

probability density. (Note that, in the case of $\beta < 1/2$ with reflection, his formulas are incorrect.) Altogether, it included four integrations, of which one, over stretched time (our τ), was taken analytically. Final results of Islah contain triple integrals to be computed numerically: integration with respect to F which originates from integrating χ^2 probability density, integration with respect to volatility V and integration with respect to parameter ξ according to the definition of the Yor function ϑ.

Drawbacks of this approach include complicated integrands, too many (three) numerical integrations, and general convergence problems with integration over ξ at small times t. Regarding the latter, we notice that explicitly real integral form for function $\vartheta(r,t)$ (4.8) contains two problematic factors, especially, for small maturities. One factor is $\sin\frac{\pi\xi}{t}$ which may oscillate very fast and another one, $e^{\frac{\pi^2}{2t}}$, may take huge values. This requires an extreme accuracy in numerical computation as discussed by Carr and Schroder [6] in the context of Asian options.

We have found ways to significantly simplify expressions for option values, coming up with a double integral of elementary functions. (It may even be considered as a single integral if we accept the heat kernel function involved,$G(t,s)$, as given – see below.) The basic idea is to transform expression (4.12) for the marginal distribution of q before integrating it with the payoff. Namely, we integrate (4.12) by parts with respect to τ, in order to get τ-time derivative $\partial_\tau p(\tau,q)$, then express $\partial_\tau p$ through the proper evolution operator using the forward Kolmogorov equation. After that, integration with payoff over F becomes trivial. Subsequent integration over stretched time τ leaves only a double integral to be computed numerically. Another essential attainment is related to integration with respect to ξ by making use of the complex (rather than real) integral form of the Yor function ϑ (4.8). Continuing the function involved into the complex plane ξ, we have managed to shift the path of integration over ξ downward from the real axis onto the horizontal line $\xi = u - i\pi$ with real u, thus converting the 'trouble making' function $\exp\{-\frac{(\xi+i\pi)^2}{2t}\}$ into the pure real and decaying exponent $\exp\{-\frac{u^2}{2t}\}$.

Leaving the derivation details to Appendix B, we present some equivalent expressions for the call option value

$$C(t,K,F_0) - (F_0-K)^+ = \sqrt{KF_0}\frac{e^{-t/8}}{\sqrt{2\pi t}}\int_0^\infty \frac{dV}{V}\left(\frac{V}{V_0}\right)^{-1/2}$$

$$\left\{\frac{1}{\pi}\int_0^\pi d\phi \frac{\sin\phi\ \sin(|\nu|\phi)}{b-\cos\phi}e^{-\frac{\xi_0(w,V)^2}{2t}} + \frac{\sin(|\nu|\pi)}{\pi}\int_0^\infty d\psi\frac{\sinh\psi}{b+\cosh\psi}e^{-|\nu|\psi}e^{-\frac{\xi_0(w,V)^2}{2t}}\right\} \tag{4.14}$$

with coefficient $b = \frac{q_K^2+q_0^2}{2q_Kq_0}$ and function

$$\xi_0(w,V) = \operatorname{arccosh}\left\{\frac{q_K^2+q_0^2+V^2+V_0^2}{2VV_0} - \frac{q_Kq_0}{VV_0}\cosh w\right\} \tag{4.15}$$

defined in the following way for two integrals

$$\begin{aligned} \cosh w = \cosh i\phi = \cos\phi \qquad & \text{for } \phi\text{-integral,} \\ \cosh w = \cosh(\pm i\pi+\psi) = -\cosh\psi \quad & \text{for } \psi\text{-integral.} \end{aligned}$$

One can get an alternative expression for the option price changing the order of integration in (4.14).

An integration over V gives rise to a heat-kernel looking function

$$G(t,s) = 2\sqrt{2}\frac{e^{-t/8}}{\sqrt{2\pi t}}\int_s^\infty d(\sqrt{\cosh u - \cosh s})e^{-\frac{u^2}{2t}} = \frac{e^{-t/8}}{\sqrt{\pi t}}\int_s^\infty du\frac{\sinh u}{\sqrt{\cosh u - \cosh s}}e^{-\frac{u^2}{2t}}. \tag{4.16}$$

Note that its derivative, $-\frac{1}{2\pi}\frac{\partial G(t,s)}{\sinh s \partial s} = G_{MK}(t,s)$, coincides with the McKean heat kernel $G_{MK}(t,s)$ on the Poincare hyperbolic plane H^2. Note also that the following alternative form of the function $G(t,s)$ obtained from (4.16) by integration by parts

$$G(t,s) = 2\sqrt{2}\frac{e^{-t/8}}{t\sqrt{2\pi t}}\int_s^\infty du\sqrt{\cosh u - \cosh s}\ \ u\, e^{-\frac{u^2}{2t}} \tag{4.17}$$

is convenient for numerical computations.

Thus, the option price looks like

$$\begin{aligned} C(t,K,F_0) - (F_0-K)^+ = \frac{1}{\pi}\sqrt{KF_0}\Bigg\{&\int_0^\pi d\phi\frac{\sin\phi\ \sin(|\nu|\phi)}{b-\cos\phi}\frac{G(t,s(w)}{D(w)} \\ &+\sin(|\nu|\pi)\int_0^\infty d\psi\frac{\sinh\psi}{b+\cosh\psi}e^{-|\nu|\psi}\frac{G(t,s(w)}{D(w)}\Bigg\}. \end{aligned} \tag{4.18}$$

Other parameters and functions involved are defined as follows:

$$\begin{aligned} D^2(w) &= \frac{2q_Kq_0}{V_0^2}(b-\cosh w)+1 \\ s(w) &= \operatorname{arccosh} D(w). \end{aligned} \tag{4.19}$$

Finally, we can simplify the option price formula using a new integration variable s

$$C(t,K,F_0) - (F_0-K)^+ = \frac{2}{\pi}\sqrt{KF_0}\left\{\int_{s_-}^{s_+} ds\frac{\sin(|\nu|\phi(s))}{\sinh s}G(t,s) + \sin(|\nu|\pi)\int_{s_+}^\infty ds\frac{e^{-|\nu|\psi(s)}}{\sinh s}G(t,s)\right\} \tag{4.20}$$

with the following underlying functions

$$\phi(s) = 2\ \arctan\sqrt{\frac{\sinh^2 s - \sinh^2 s_-}{\sinh^2 s_+ - \sinh^2 s}} \tag{4.21}$$

$$\psi(s) = 2\,\operatorname{arctanh}\sqrt{\frac{\sinh^2 s - \sinh^2 s_+}{\sinh^2 s - \sinh^2 s_-}} \tag{4.22}$$

the integration limits

$$s_- = \operatorname{arcsinh}\left(\frac{|q_K - q_0|}{V_0}\right) \tag{4.23}$$

$$s_+ = \operatorname{arcsinh}\left(\frac{q_K + q_0}{V_0}\right) \tag{4.24}$$

and the Kernel function $G(t,s)$ given by (4.16).

4.3 Asymptotics at large strikes

Full calculation of asymptotics for large strikes turned out to be complicated and will be addressed elsewhere; here we give its leading term.

The dominating term in the option price integrand (4.20) is the kernel $G(t,s)$ with strongly decreasing Gaussian asymptotics. Indeed, make in (4.16) a substitution

$$u = \sqrt{s^2+w^2} \simeq s\left(1+\frac{w^2}{2s^2}\right) = s + \frac{w^2}{2s}.$$

Then

$$\cosh u \simeq \cosh s + \frac{w^2}{2s}\sinh s$$
$$\sqrt{\cosh u - \cosh s} \simeq \sqrt{\frac{\sinh s}{2s}}\, w\left(1+O(s^{-1})\right)$$

and the asymptotic of $G(t,s)$ looks like

$$G(t,s) = 2\sqrt{2}\sqrt{\frac{\sinh s}{2s}}\frac{e^{-t/8}}{\sqrt{2\pi t}}\int_0^\infty dw\; e^{-\frac{s^2+w^2}{2t}}\left(1+O(s^{-1})\right) = \sqrt{\frac{\sinh s}{s}}e^{-\frac{s^2}{2t}-\frac{t}{8}}\left(1+O(s^{-1})\right). \qquad (4.25)$$

The leading asymptotics of the option price comes from the term $G(t,s)$ corresponding to large $s \sim s_- \sim s_+$ which, for simplicity, we define as

$$s_0 = \ln\frac{2\,q_K}{V_0}. \qquad (4.26)$$

We see that the resulting leading asymptotics

$$C(t,K,F_0) \sim G(t,s_0) \sim e^{-\frac{s_0^2}{2t}} \quad \text{for} \quad K\to\infty \qquad (4.27)$$

coincide with that given by the Heat-Kernel small time expansion (2.20) where, for large strikes, $s_{\min} \sim s_0$. We doubt, however, that the pre-exponential factors of these two different limits, $K\to\infty$ and $t\to 0$, will also coincide.

Given the Gaussian nature of the decay we can quantify large s_0 as being

$$s_0 \sim 3\sqrt{t} \qquad (4.28)$$

or, in terms of the q_K,

$$q_K \sim V_0 e^{3\sqrt{t}} \qquad (4.29)$$

or, in terms of the strikes,

$$K \sim \left((1-\beta)\,V_0\right)^{\frac{1}{1-\beta}}\, e^{\frac{3\sqrt{t}}{1-\beta}}. \qquad (4.30)$$

5 Heat-kernel expansion for SABR density

The heat-kernel expansion (DeWitt (1965)) is a small-time approximation for the probability density function (PDF). This is a regular recipe for general stochastic systems (see the review of Avramidi [4]). The PDF expansion for the SABR model was calculated in Henry-Labordere (2008) and Paulot (2009). It can be written in our (q, V) variables (2.5) as[9]

$$p(q,v) = \frac{1}{\gamma v^2 \sqrt{1-\rho^2}} \frac{1}{2\pi t} \sqrt{\frac{s(q,v)}{\sinh s(q,v)}} \mathcal{P}(q,v)\; e^{-\frac{s^2(q,v)}{2\gamma^2 t}} (1 + O(t)) \tag{5.1}$$

where *geodesic distance* $s(q, v)$ from the leading term depends on the volatility of the processes Q_t and v_t, and parallel transport $\mathcal{P}(q, v)$ depends on the drifts.

Before proceeding with details, we notice that the distance and the parallel transport do not depend on time. It is also worth mentioning that the heat kernel does not take into account the boundary conditions: for small time, the rate "cannot" approach the boundary.

In principal, it is possible to obtain the higher orders in time[10], however, the formulas are very complicated (see Paulot (2009)).

To define the distance and the parallel transport, we introduce new variables (on the so-called hyperbolic plane)

$$x = \frac{q - \frac{v}{\gamma}\cos\alpha}{\sin\alpha} \tag{5.2}$$

$$y = \frac{v}{\gamma} \tag{5.3}$$

with

$$\rho = \cos\alpha. \tag{5.4}$$

The distance s is defined in terms of the variables (x, y) as

$$\cosh s = \frac{(x-x_0)^2 + (y-y_0)^2}{2yy_0} + 1$$

or in terms of (q, v)

$$\cosh s = \frac{[\gamma\delta q - \rho(v-v_0)]^2}{2(1-\rho^2)v\, v_0} + \frac{(v-v_0)^2}{2vv_0} + 1. \tag{5.5}$$

Proceed now to the parallel transport, also defined by its logarithm $\mathcal{A}$

$$\mathcal{P} = e^{-\mathcal{A}}.$$

Loosely speaking, the term $\mathcal{A}$ is an integral of the system drift over the most probable path connecting initial point (q_0, v_0) and final point (q, v). Detailed consideration permits one to express the parallel transport as

$$\mathcal{A} = -(\nu + 1/2)\ln\left(\frac{q}{q_0}\right) + \mathcal{B} = \frac{1}{2}\ln\left(\frac{F}{F_0}\right)^{\beta} + \mathcal{B} \tag{5.6}$$

[9] The element of probability is defined as $dP = p(q, v)\, dq\, dv$.

[10] Presented here as $O(t)$

where $\mathcal{B}$ is the following integral

$$\mathcal{B} = -\tfrac{1}{2}\frac{\beta}{1-\beta}\frac{\rho}{(1-\rho^2)}\int_C \frac{-\rho dq' + dV'}{q'} \tag{5.7}$$

along the geodesic line C from original to current point, i.e., the most probable path.

It occurs that the geodesic line is a semi-circle in coordinates (x, y) with center $(x_c, 0)$

$$x_c = \frac{x + x_0}{2} + \frac{y^2 - y_0^2}{2(x - x_0)} \tag{5.8}$$

and radius R

$$R^2 = \frac{\left[(x-x_0)^2 + y^2 + y_0^2\right]^2 - 4y^2y_0^2}{4(x-x_0)^2}. \tag{5.9}$$

The curve C is parameterized via the angle on the circle, i.e. a point (x', y') lying on the geodesic line is expressed via the angle φ'

$$\begin{aligned} x' &= x_c + R\cos\varphi' \\ y' &= R\sin\varphi'. \end{aligned}$$

The angles corresponding to the initial (x_0, y_0) and final points (x, y) are

$$\begin{aligned} \varphi &= \arccos\frac{x - x_c}{R} \\ \varphi_0 &= \arccos\frac{x_0 - x_c}{R} \end{aligned}$$

and satisfy

$$0 \le \varphi_0 \le \varphi' \le \varphi \le \pi. \tag{5.10}$$

The integral $\mathcal{B}$ (5.7) can be transformed to

$$\mathcal{B} = \tfrac{1}{2}\frac{\beta}{1-\beta}\cot\alpha\int_C \frac{-\cos\alpha\ dx' + \sin\alpha\ dy'}{q_0 + (x'-x_0)\sin\alpha + (y'-y_0)\cos\alpha} \tag{5.11}$$

$$= -\tfrac{1}{2}\frac{\beta}{1-\beta}\cot\alpha\int_{\varphi_0}^{\varphi} \frac{R\sin(\varphi'+\alpha)\ d\varphi'}{q_0 - R\sin(\varphi_0+\alpha) + R\sin(\varphi'+\alpha)}. \tag{5.12}$$

Finally, denoting

$$L^{-1} = \frac{q_0}{R} - \sin(\varphi_0 + \alpha) = \frac{x_c\ \sin\alpha}{R}, \tag{5.13}$$

we conclude that

$$\mathcal{B} = -\tfrac{1}{2}\frac{\beta}{1-\beta}\cot\alpha\left(\varphi - \varphi_0 - \int_{\varphi_0+\alpha}^{\varphi+\alpha}\frac{d\varphi'}{1 + L\sin\varphi'}\right). \tag{5.14}$$

Note that this integral can be easily taken analytically as explained in the next section.

6 General correlation approximation formulas

In this Section we will apply the mapping technique (see Antonov-Misirpashaev (2009)) which works as follows. To approximate an option price $\mathcal{C}(T,K)=\mathbb{E}[(F_T-K)^+]$ we come up with another *mimicking model* or *proxy* $\tilde{F}_t$, having the same small time expansion for the option. The mimicking model is supposed to have an exact expression for its option price. The final result is calculated using the mimicking model

$$\mathcal{C}(T,K)\simeq\mathbb{E}[(\tilde{F}_T-K)^+].$$

For example, Hagan used the Black-Scholes model or normal one for this. Paulot has proposed the CEV model as the mimicking model. We will go further and use the SABR model with zero correlation (SABR ZC) having similar characteristics and asymptotics to the initial SABR model.

First, we represent the SABR rate PDF using the BES SV PDF (5.1)

$$P(t;\,F,v)\simeq\frac{1}{2\pi t\gamma}\frac{1}{v^2F^\beta\sqrt{1-\rho^2}}\sqrt{\frac{s}{\sinh s}}\mathcal{P}\,e^{-\frac{s^2}{2t\gamma^2}}. \tag{6.1}$$

Then, we apply Ito's lemma to a process $(F_t-K)^+$ which gives, after averaging,

$$E[(F_T-K)^+]=(F_0-K)^++\frac{1}{2}\int_0^T dtE[\delta(F_t-K)\,F_t^{2\beta}\,v_t^2]. \tag{6.2}$$

The average under the integral can be rewritten as

$$E[\delta(F_t-K)\,F_t^{2\beta}\,v_t^2]=K^{2\beta}\int dv\,P(t;\,K,v)\,v^2 \tag{6.3}$$

and taken using the saddle point for small times

$$\int dv\,f(v)\,e^{-\frac{s^2(F_0,v_0;K,v)}{2t\gamma^2}}\simeq\gamma\sqrt{2\pi t(1-\rho^2)v_0v_{\min}}\sqrt{\frac{\sinh s_{\min}}{s_{\min}}}e^{-\frac{s_{\min}^2}{2t\gamma^2}}\,f(v_{\min}) \tag{6.4}$$

where

$$v_{\min}^2=\delta q^2\,\gamma^2+2\rho\delta q\,\gamma\,v_0+v_0^2 \tag{6.5}$$

and

$$s_{\min}=\left|\ln\frac{v_{\min}+\rho v_0+\delta q\,\gamma}{(1+\rho)v_0}\right| \tag{6.6}$$

for

$$\delta q=\frac{1}{1-\beta}\left(K^{1-\beta}-F_0^{1-\beta}\right). \tag{6.7}$$

Thus,

$$E[\delta(F_t-K)\,F_t^{2\beta}\,v_t^2]=\frac{1}{\sqrt{2\pi t}}\,K^\beta\,\sqrt{v_0v_{\min}}\,e^{-\frac{s_{\min}^2}{2t\gamma^2}}\,\mathcal{P}_{\min} \tag{6.8}$$

where

$$\mathcal{P}_{\min}=\mathcal{P}_{\min}(F_0,v_0;K,v_{\min}). \tag{6.9}$$

The integration over time (6.2) can be done analytically. Indeed, for small T,

$$\int_0^T dt \frac{e^{-\frac{1}{2}\frac{s^2}{t\gamma^2}}}{\sqrt{t}} = 2\,s\,\gamma^{-1}\int_{\frac{s}{\gamma\sqrt{T}}}^{\infty}\frac{dx}{x^2}\,e^{-\frac{1}{2}x^2} \simeq \gamma^2\frac{T^{\frac{3}{2}}}{\frac{s^2}{2}}\,e^{-\frac{1}{2}\frac{s^2}{T\gamma^2}}. \tag{6.10}$$

Thus, the option time-value

$$\mathcal{O}(T,K) = \frac{T^{\frac{3}{2}}}{2\sqrt{2\pi}}\,\exp\left\{-\frac{1}{2}\frac{s_{\min}^2}{T\gamma^2} - \ln\frac{s_{\min}^2}{2\gamma^2} + \ln\left(K^\beta\sqrt{v_0 v_{\min}}\right) - \mathcal{A}_{\min}\right\}. \tag{6.11}$$

The integral term $\mathcal{B}_{\min}$ in the parallel transport (5.6)

$$\mathcal{A}_{\min} = \frac{1}{2}\ln\left(\frac{K}{F_0}\right)^\beta + \mathcal{B}_{\min} \tag{6.12}$$

simplifies when $v = v_{\min}$. Indeed,

$$\phi + \alpha = \pi \tag{6.13}$$

which is equivalent to

$$q = x_c\sin\alpha \tag{6.14}$$

or

$$y = R\sin\alpha. \tag{6.15}$$

The parameter L can be also simplified:

$$L = \frac{y}{q\,\sin\alpha} = \frac{v_{\min}}{q\,\gamma\,\sin\alpha}. \tag{6.16}$$

Then the parallel transport integral (5.14) transforms to

$$\mathcal{B}_{\min} = \int B_i dx^i = -\tfrac{1}{2}\frac{\beta}{1-\beta}\cot\alpha\left(\pi - \varphi_0 - \alpha - \int_{\varphi_0+\alpha}^{\pi}\frac{d\varphi'}{1+L\sin\varphi'}\right). \tag{6.17}$$

The underlying integral can be easily taken analytically. Indeed, after variable change $u = \cot\frac{\varphi'}{2}$, we have

$$I \equiv \int_{\varphi_0+\alpha}^{\pi}\frac{d\varphi'}{1+L\sin\varphi'} = \int_0^{u_0}\frac{du}{1+u^2+2\,L\,u} \tag{6.18}$$

where we used relations $\sin\varphi' = 2u/(1+u^2)$ and $d\varphi' = -2du/(1+u^2)$ and denoted

$$u_0 = \cot\tfrac{\varphi_0+\alpha}{2}.$$

The latter integral reads

$$I = \begin{cases} \frac{2}{\sqrt{1-L^2}}\left(\arctan\frac{u_0+L}{\sqrt{1-L^2}} - \arctan\frac{L}{\sqrt{1-L^2}}\right) & \text{for } L<1, \\ \frac{1}{\sqrt{L^2-1}}\ln\frac{u_0\left(L+\sqrt{L^2-1}\right)+1}{u_0\left(L-\sqrt{L^2-1}\right)+1} & \text{for } L>1. \end{cases} \tag{6.19}$$

Note that we can express the underlying parameter u_0 in simple terms

$$u_0 = \cot \tfrac{\varphi_0+\alpha}{2} = \frac{\delta q\,\gamma\rho + v_0 - v_{\min}}{\delta q\,\gamma\sqrt{1-\rho^2}}$$

using

$$\sin(\varphi_0+\alpha) = -\frac{\delta q}{R} \quad \text{and} \quad \cos(\varphi_0+\alpha) = -\frac{\delta q\,\cos\alpha + v_0}{R\sin\alpha}. \tag{6.20}$$

6.1 Map to the CEV model

We describe here how to do the map to the CEV model (see also Paulot (2009)). First, calculate the time-value expansion of the CEV mimicking model,

$$d\tilde{F} = \tilde{F}^{\beta'}\sigma d\tilde{W}, \tag{6.21}$$

with possibly different power β' with respect to the SABR power. The CEV PDF expansion reads (see, for example, Jeanblanc et al. (2009))

$$p_{CEV}(t,F) \equiv E[(\tilde{F}_t - F)] = \frac{1}{\sqrt{2\pi\,t\,\sigma^2}}\,F^{-\beta'}\,e^{-\frac{\left(F^{1-\beta'}-F_0^{1-\beta'}\right)^2}{2\,t\,\sigma^2(1-\beta')^2}}\left(\frac{F}{F_0}\right)^{-\frac{\beta'}{2}}. \tag{6.22}$$

The integrand underlying the option price

$$E[(\tilde{F}_T - K)^+] = (F_0-K)^+ + \frac{1}{2}\int_0^T dt E[\delta(\tilde{F}_t - K)\,\tilde{F}_t^{2\beta'}\,\sigma^2] \tag{6.23}$$

is simply

$$E[\delta(\tilde{F}_t - K)\,F_t^{2\beta'}\,\sigma^2] \simeq \frac{\sigma^2}{\sqrt{2\pi\,t\,\sigma^2}}\,e^{-\frac{\left(K^{1-\beta'}-F_0^{1-\beta'}\right)^2}{2\,t\,\sigma^2(1-\beta')^2}}\,(K\,F_0)^{\frac{\beta'}{2}} \tag{6.24}$$

where CEV geodesic distance is

$$s_{CEV} = \frac{K^{1-\beta'} - F_0^{1-\beta'}}{1-\beta'}. \tag{6.25}$$

The option time-value can be calculated as follows

$$\begin{aligned}
\tilde{\mathcal{O}}(T,K) &\equiv \frac{1}{2}\int_0^T dt E[\delta(\tilde{F}_t - K)\,F_t^{2\beta'}\,\sigma^2] \simeq \frac{1}{2}\sigma^2\,(K\,F_0)^{\frac{\beta'}{2}}\int_0^T dt\frac{1}{\sqrt{2\pi\,t\,\sigma^2}}\,e^{-\frac{s_{CEV}^2}{2\,t\,\sigma^2}} && (6.26)\\
&= \frac{1}{2}\sigma^2\,(K\,F_0)^{\frac{\beta'}{2}}\int_0^T dt\frac{1}{\sqrt{2\pi\,t\,\sigma^2}}\,e^{-\frac{s_{CEV}^2}{2\,t\,\sigma^2}} && (6.27)\\
&\simeq \frac{T^{\frac{3}{2}}}{2\sqrt{2\pi}}\,\exp\left\{-\frac{1}{2}\frac{s_{CEV}^2}{T\,\sigma^2} + \ln\sigma - \ln\frac{s_{CEV}^2}{2\,\sigma^2} + \frac{\beta'}{2}\ln(K\,F_0)\right\}. && (6.28)
\end{aligned}$$

To make a fit with SABR, we should equate

$$\frac{1}{2}\frac{s_{CEV}^2}{T\,\sigma^2} - \ln\sigma + \ln\frac{s_{CEV}^2}{2\,\sigma^2} - \frac{\beta'}{2}\ln(K\,F_0) = \frac{1}{2}\frac{s_{\min}^2}{T\gamma^2} + \ln\frac{s_{\min}^2}{2\gamma^2} - \ln\left(K^{\beta}\sqrt{v_0 v_{\min}}\right) + \mathcal{A}_{\min}. \tag{6.29}$$

Consider now expansion of the CEV volatility

$$\sigma = \sigma_0 + T\sigma_1 + \cdots$$

We obtain the following condition, zeroing T^{-1} coefficients

$$\frac{s^2_{CEV}}{T\,\sigma^2} = \frac{s^2_{\min}}{T\gamma^2} \quad \Rightarrow \quad \sigma = \gamma \frac{s_{CEV}}{s_{\min}}. \tag{6.30}$$

Expanding σ in $\frac{s^2_{CEV}}{T\,\sigma^2}$, we get a condition for free terms equal to zero

$$-\frac{s^2_{CEV}}{\sigma_0^2}\,\frac{\sigma_1}{\sigma_0} - \ln\sigma_0 - \frac{\beta'}{2}\ln\left(K\,F_0\right) = -\ln\left(K^\beta\,\sqrt{v_0 v_{\min}}\right) + \mathcal{A}_{\min} \tag{6.31}$$

giving the CEV volatility correction

$$\frac{\sigma_1}{\sigma_0} = \frac{\ln\left(K^\beta\,\sqrt{v_0 v_{\min}}\right) - \mathcal{A}_{\min} - \ln\sigma_0 - \frac{\beta'}{2}\ln\left(K\,F_0\right)}{\frac{s^2_{CEV}}{\sigma_0^2}}. \tag{6.32}$$

To obtain the effective BS volatility expansion, we should calculate the limit $\beta' \to 1$. The BS geodesic distance reads

$$s_{BS} = s_{CEV}|_{\beta'=1} = \left|\ln\frac{K}{F_0}\right|$$

giving the leading volatility term

$$\sigma_0 = \gamma\frac{\left|\ln\frac{K}{F_0}\right|}{s_{\min}}$$

and the first volatility correction

$$\frac{\sigma_1}{\sigma_0} = \frac{\ln\left(K^\beta\,\sqrt{v_0 v_{\min}}\right) - \mathcal{A}_{\min} - \ln\sigma_0 - \frac{1}{2}\ln\left(K\,F_0\right)}{\frac{s^2_{\min}}{\gamma^2}}.$$

In the ATM limit the effective BS volatility expansion terms read

$$\sigma_0|_{K=F_0} = v_0\,F_0^{\beta-1}$$

and

$$\left.\frac{\sigma_1}{\sigma_0}\right|_{K=F_0} = \frac{1}{24}\,v_0^2(1-\beta)^2\,F_0^{2\beta-2} + \frac{1}{4}v_0\,\rho\,\gamma\,\beta\,F_0^{\beta-1} + \frac{1}{12}\gamma^2 - \frac{1}{8}\rho^2\gamma^2$$

Note that Hagan et al. (2002) has calculated the BS volatility expansion using heuristic methods effectively assuming close to the ATM strikes (see Paulot (2009)).

6.2 Map to the zero correlation SABR model

Zero correlation SABR process represents a better choice of the mimicking model (proxy). Indeed, it has close properties with a general correlation SABR and possesses an analytical solution for option price. Denote the mimicking model parameters with a tilde (2.37-2.38). To find them, we should match the option price expansion (6.11) between the initial SABR and its zero correlation proxy

$$\frac{1}{2}\frac{\tilde{s}^2_{\min}}{T\tilde{\gamma}^2}+\ln\frac{\tilde{s}^2_{\min}}{2\tilde{\gamma}^2}-\ln\left(K^{\tilde{\beta}}\sqrt{\tilde{v}_0\tilde{v}_{\min}}\right)+\tilde{\mathcal{A}}_{\min}=\frac{1}{2}\frac{s^2_{\min}}{T\gamma^2}+\ln\frac{s^2_{\min}}{2\gamma^2}-\ln\left(K^{\beta}\sqrt{v_0 v_{\min}}\right)+\mathcal{A}_{\min}. \tag{6.33}$$

We fix the vol-of-vol $\tilde{\gamma}$ and the power $\tilde{\beta}$ in the mimicking model and look for time-expansion of the initial volatility

$$\tilde{v}_0=\tilde{v}_0^{(0)}+T\,\tilde{v}_0^{(1)}+\cdots \tag{6.34}$$

Denote the function appearing in the argument of the logarithm of the optimal geodesic distance (6.6) as

$$\phi=\frac{v_{\min}+\rho v_0+\gamma\delta q}{(1+\rho)v_0}, \tag{6.35}$$

i.e., $s_{\min}=|\ln\phi|$. Similarly, for the zero correlation, $\tilde{s}_{\min}(\tilde{v}_0)=|\ln\tilde{\phi}(\tilde{v}_0)|$, we have

$$\tilde{\phi}(\tilde{v}_0)=\sqrt{1+\left(\frac{\delta\tilde{q}\,\tilde{\gamma}}{\tilde{v}_0}\right)^2}+\frac{\delta\tilde{q}\,\tilde{\gamma}}{\tilde{v}_0} \tag{6.36}$$

where

$$\delta\tilde{q}=\frac{K^{1-\tilde{\beta}}-F_0^{1-\tilde{\beta}}}{1-\tilde{\beta}}.$$

To organize the fit (6.33) in the main order, we should find the leading order of the mimicking-model initial volatility (6.34) such that the equation

$$\frac{1}{2}\frac{\tilde{s}^2_{\min}\left(\tilde{v}_0^{(0)}\right)}{T\tilde{\gamma}^2}=\frac{1}{2}\frac{s^2_{\min}}{T\gamma^2} \tag{6.37}$$

is satisfied. A solution of this equation follows from the fit condition $\tilde{\phi}\left(\tilde{v}_0^{(0)}\right)=\phi^{\frac{\tilde{\gamma}}{\gamma}}$

$$\tilde{v}_0^{(0)}=\frac{2\,\Phi\,\delta\tilde{q}\,\tilde{\gamma}}{\Phi^2-1} \tag{6.38}$$

where we have denoted $\Phi=\phi^{\frac{\tilde{\gamma}}{\gamma}}$. To calculate its first correction, we notice that the mimicking-model parallel transport does not depend on the initial volatility (2.24-2.25) due to zero correlation

$$\tilde{\mathcal{A}}_{\min}=\frac{1}{2}\ln(K/F_0)^{\tilde{\beta}}. \tag{6.39}$$

Then, expand in time the square of the optimal distance of the mimicking model

$$\frac{1}{2}\tilde{s}^2_{\min}\left(\tilde{v}_0^{(0)}+T\,\tilde{v}_0^{(1)}\right)=\frac{1}{2}\tilde{s}^2_{\min}\left(\tilde{v}_0^{(0)}\right)-\Omega\,T\,\frac{\tilde{v}_0^{(1)}}{\tilde{v}_0^{(0)}}+\cdots \tag{6.40}$$

where the derivative coefficient reads

$$\Omega = \frac{\Phi^2 - 1}{\Phi^2 + 1} \ln \Phi. \tag{6.41}$$

Substituting this into (6.33), we obtain a fit equation for the free terms in time

$$-\frac{\Omega\, \tilde{v}_0^{(1)}}{\tilde{\gamma}^2\, \tilde{v}_0^{(0)}} - \ln\left(K^{\tilde{\beta}} \sqrt{\tilde{v}_0^{(0)} \tilde{v}_{\min}^{(0)}}\right) + \tilde{\mathcal{A}}_{\min} = -\ln\left(K^{\beta} \sqrt{v_0 v_{\min}}\right) + \mathcal{A}_{\min} \tag{6.42}$$

where the optimal point volatility can be further simplified

$$\tilde{v}_{\min}^{(0)} = \sqrt{\delta\tilde{q}^2\, \tilde{\gamma}^2 + \tilde{v}_0^{(0)\,2}} = \tilde{v}_0^{(0)}\, \frac{\Phi^2 + 1}{2\,\Phi}. \tag{6.43}$$

This immediately gives us the correction to the initial volatility

$$\frac{\tilde{v}_0^{(1)}}{\tilde{v}_0^{(0)}} = \tilde{\gamma}^2\, \frac{\ln\left(K^{\beta} \sqrt{v_0 v_{\min}}\right) - \ln\left(K^{\tilde{\beta}} \sqrt{\tilde{v}_0^{(0)} \tilde{v}_{\min}^{(0)}}\right) + \tilde{\mathcal{A}}_{\min} - \mathcal{A}_{\min}}{\Omega} \tag{6.44}$$

which reduces to (2.32) after substitution (6.12).

The effective zero correlation initial volatility depends on a choice of the fixed parameters $\tilde{\beta}$ and $\tilde{\gamma}$. A good choice based primarily on our numerical experiments reduces to

$$\tilde{\beta} = \beta, \tag{6.45}$$

$$\tilde{\gamma}^2 = \gamma^2 - \frac{3}{2}\left\{\gamma^2\rho^2 + \sigma_{BS}(F_0)\,\gamma\rho\,(1-\beta)\right\}, \tag{6.46}$$

where effective BS ATM implied volatility $\sigma_{BS}(F_0) = v_0\, F_0^{\beta-1}$. The intuition behind our choice is the following: The same power β helps with asymptotics for small strikes. The vol-of-vol $\tilde{\gamma}$ choice is inspired by a fit of the ATM implied volatility curvature.

An ATM case of the effective volatility (6.38) and its correction (6.44) corresponding to a limit $K \to F_0$. is described in Appendix C.

7 Numerical experiments

In this section, we demonstrate the efficiency of our approach. We analyze a wide variety of model coefficients for large maturities. The data are summarized in the table below

Rate Initial Value	F_0	1
SV Initial Value	v_0	0.25
Vol-of-Vol	γ	0.3
Correlations	ρ	$-0.8,\ -0.5,\ -0.2$
Skews	β	0.3, 0.6, 0.9
Maturities	T	10Y and 20Y

We present the Black-Scholes implied volatility for European call options $\mathcal{C}(T,K) = E[(F_T - K)^+]$ for a large range of strikes K and as well as second-moment underlying CMS calculations.

CMS convexity adjustments depend on the second moment of the rate process, which can be evaluated by the usual static replication formula (Hagan (2003))

$$E\left[F_T^2\right] = 2\int_0^\infty dK\, E[(F_T - K)^+]. \tag{7.1}$$

For the SABR ZC Map option approximation, one can use this formula directly for the second moment calculations without any heuristic tricks (e.g., strike domain limitations, tail replacements, etc.). The tiny negativity of certain density approximations for the SABR ZC Map does not influence the quality of the CMS calculations. Note that, for close-to-zero correlations and large skews, the big-strike tail is very fat, which produces a very slow convergence of the static replication integral.

In our numerical experiments, we compare the following methods:

- Monte Carlo simulation (**MC**)
- The Henry-Labordere (2008) and Paulot (2009) (**HL-P**) form of the implied volatility expansion (regular leading order and the first correction)
- The Hagan et al. (2002) form of the implied volatility expansion (**Hagan**)
- Map to the zero correlation SABR model (**ZC Map**) (regular leading order (2.31) and the first correction (2.32))
- Hybrid map to the zero correlation SABR model (**Hyb ZC Map**) (regular leading order (2.31) and the ATM first correction (2.34))

	Value (%)					Difference (bps)			
K	MC	HL-P	Hagan	ZC Map	Hyb ZC Map	HL-P	Hagan	ZC Map	Hyb ZC Map
0.1	57.15	78.98	71.76	57.44	59.78	2183	1461	29	263
0.2	48.18	59.92	57.25	48.43	50.18	1174	907	25	200
0.3	42.45	49.99	48.86	42.66	44.03	754	641	21	158
0.4	38.14	43.39	42.93	38.33	39.39	525	479	19	125
0.5	34.65	38.49	38.35	34.83	35.65	384	370	18	100
0.6	31.7	34.61	34.62	31.89	32.49	291	292	19	79
0.7	29.15	31.41	31.48	29.34	29.77	226	233	19	62
0.8	26.89	28.69	28.76	27.09	27.36	180	187	20	47
0.9	24.87	26.34	26.38	25.09	25.22	147	151	22	35
1	**23.04**	**24.27**	**24.27**	**23.29**	**23.29**	**123**	**123**	**25**	**25**
1.1	21.39	22.44	22.38	21.66	21.54	105	99	27	15
1.2	19.89	20.8	20.68	20.19	19.97	91	79	30	8
1.3	18.54	19.36	19.16	18.87	18.55	82	62	33	1
1.4	17.32	18.08	17.81	17.69	17.29	76	49	37	-3
1.5	16.25	16.97	16.63	16.66	16.18	72	38	41	-7
1.6	15.33	16.02	15.62	15.77	15.23	69	29	44	-10
1.7	14.55	15.23	14.78	15.04	14.44	68	23	49	-11
1.8	13.91	14.6	14.12	14.44	13.81	69	21	53	-10
1.9	13.4	14.11	13.6	13.98	13.32	71	20	58	-8
2	13.01	13.73	13.22	13.62	12.96	72	21	61	-5

Table 1: Implied vol and its error for different methods, 10Y maturity, $\beta = 0.3$, $\rho = -0.8$.

	Value (%)					Difference (bps)			
K	MC	HL-P	Hagan	ZC Map	Hyb ZC Map	HL-P	Hagan	ZC Map	Hyb ZC Map
0.1	51.23	56.44	55.18	51.14	54.91	521	395	-9	368
0.2	43.22	46.25	46.15	43.25	45.83	303	293	3	261
0.3	38.27	40.37	40.59	38.35	40.24	210	232	8	197
0.4	34.63	36.22	36.52	34.74	36.14	159	189	11	151
0.5	31.73	33	33.3	31.87	32.89	127	157	14	116
0.6	29.3	30.36	30.62	29.46	30.2	106	132	16	90
0.7	27.22	28.12	28.32	27.39	27.89	90	110	17	67
0.8	25.39	26.17	26.31	25.58	25.88	78	92	19	49
0.9	23.76	24.46	24.53	23.97	24.11	70	77	21	35
1	**22.29**	**22.93**	**22.93**	**22.52**	**22.52**	**64**	**64**	**23**	**23**
1.1	20.96	21.56	21.49	21.21	21.09	60	53	25	13
1.2	19.76	20.33	20.18	20.03	19.82	57	42	27	6
1.3	18.67	19.22	19.01	18.97	18.67	55	34	30	0
1.4	17.7	18.24	17.96	18.02	17.66	54	26	32	-4
1.5	16.83	17.37	17.03	17.19	16.77	54	20	36	-6
1.6	16.07	16.62	16.22	16.46	16	55	15	39	-7
1.7	15.42	15.98	15.54	15.84	15.36	56	12	42	-6
1.8	14.87	15.45	14.98	15.32	14.84	58	11	45	-3
1.9	14.43	15.01	14.54	14.9	14.42	58	11	47	-1
2	14.07	14.66	14.19	14.56	14.11	59	12	49	4

Table 2: Implied vol and its error for different methods, 10Y maturity, $\beta = 0.6$, $\rho = -0.8$.

	Value (%)					Difference (bps)			
K	MC	HL-P	Hagan	ZC Map	Hyb ZC Map	HL-P	Hagan	ZC Map	Hyb ZC Map
0.1	43.43	43.21	45.3	42.69	46.1	-22	187	-74	267
0.2	37.42	37.29	38.73	36.92	39.16	-13	131	-50	174
0.3	33.72	33.63	34.71	33.35	34.94	-9	99	-37	122
0.4	30.98	30.93	31.75	30.7	31.87	-5	77	-28	89
0.5	28.79	28.77	29.39	28.58	29.43	-2	60	-21	64
0.6	26.95	26.96	27.42	26.79	27.41	1	47	-16	46
0.7	25.37	25.4	25.72	25.26	25.67	3	35	-11	30
0.8	23.97	24.03	24.23	23.9	24.16	6	26	-7	19
0.9	22.72	22.81	22.9	22.69	22.81	9	18	-3	9
1	**21.6**	**21.71**	**21.71**	**21.61**	**21.61**	**11**	**11**	**1**	**1**
1.1	20.58	20.72	20.63	20.63	20.53	14	5	5	-5
1.2	19.66	19.82	19.66	19.74	19.55	16	0	8	-11
1.3	18.83	19.02	18.78	18.95	18.69	19	-5	12	-14
1.4	18.09	18.3	18	18.24	17.91	21	-9	15	-18
1.5	17.43	17.66	17.3	17.61	17.23	23	-13	18	-20
1.6	16.84	17.11	16.7	17.06	16.65	27	-14	22	-19
1.7	16.34	16.63	16.18	16.58	16.15	29	-16	24	-19
1.8	15.91	16.22	15.75	16.18	15.73	31	-16	27	-18
1.9	15.55	15.88	15.4	15.84	15.4	33	-15	29	-15
2	15.26	15.6	15.12	15.56	15.14	34	-14	30	-12

Table 3: Implied vol and its error for different methods, 10Y maturity, $\beta = 0.9$, $\rho = -0.8$.

	Value (%)					Difference (bps)			
K	MC	Pauloty	Hagan	ZC Map	Hyb ZC Map	HL-P	Hagan	ZC Map	Hyb ZC Map
0.1	55.93	76.42	72.71	55.01	56.81	2049	1678	-92	88
0.2	47.12	58.49	57.68	46.39	47.82	1137	1056	-73	70
0.3	41.58	49.13	49.17	41	42.15	755	759	-58	57
0.4	37.48	42.93	43.27	37.02	37.96	545	579	-46	48
0.5	34.22	38.37	38.78	33.86	34.62	415	456	-36	40
0.6	31.52	34.81	35.19	31.25	31.84	329	367	-27	32
0.7	29.24	31.92	32.22	29.05	29.48	268	298	-19	24
0.8	27.27	29.52	29.72	27.17	27.45	225	245	-10	18
0.9	25.56	27.5	27.6	25.54	25.68	194	204	-2	12
1	**24.08**	**25.79**	**25.79**	**24.14**	**24.14**	**171**	**171**	**6**	**6**
1.1	22.8	24.34	24.24	22.93	22.8	154	144	13	0
1.2	21.7	23.11	22.93	21.9	21.65	141	123	20	-5
1.3	20.77	22.08	21.84	21.04	20.67	131	107	27	-10
1.4	19.98	21.23	20.93	20.31	19.86	125	95	33	-12
1.5	19.33	20.53	20.2	19.72	19.18	120	87	39	-15
1.6	18.8	19.96	19.62	19.24	18.64	116	82	44	-16
1.7	18.37	19.51	19.16	18.86	18.21	114	79	49	-16
1.8	18.04	19.16	18.82	18.57	17.88	112	78	53	-16
1.9	17.77	18.88	18.56	18.34	17.63	111	79	57	-14
2	17.57	18.67	18.37	18.16	17.44	110	80	59	-13

Table 4: Implied vol and its error for different methods, 10Y maturity, $\beta = 0.3$, $\rho = -0.5$.

	Value (%)					Difference (bps)			
K	MC	HL-P	Hagan	ZC Map	Hyb ZC Map	HL-P	Hagan	ZC Map	Hyb ZC Map
0.1	50.05	56.54	57.09	48.98	51.85	649	704	-107	180
0.2	42.32	46.41	47.43	41.65	43.75	409	511	-67	143
0.3	37.63	40.66	41.65	37.18	38.8	303	402	-45	117
0.4	34.24	36.66	37.52	33.94	35.2	242	328	-30	96
0.5	31.59	33.62	34.32	31.4	32.38	203	273	-19	79
0.6	29.42	31.18	31.73	29.33	30.06	176	231	-9	64
0.7	27.61	29.18	29.57	27.6	28.11	157	196	-1	50
0.8	26.07	27.5	27.75	26.13	26.46	143	168	6	39
0.9	24.75	26.08	26.19	24.88	25.03	133	144	13	28
1	**23.61**	**24.87**	**24.87**	**23.82**	**23.82**	**126**	**126**	**21**	**21**
1.1	22.65	23.85	23.75	22.91	22.78	120	110	26	13
1.2	21.83	22.99	22.8	22.15	21.91	116	97	32	8
1.3	21.14	22.28	22.02	21.52	21.18	114	88	38	4
1.4	20.57	21.69	21.38	21	20.58	112	81	43	1
1.5	20.11	21.21	20.87	20.57	20.11	110	76	46	0
1.6	19.73	20.83	20.48	20.24	19.73	110	75	51	0
1.7	19.44	20.53	20.18	19.98	19.45	109	74	54	1
1.8	19.21	20.3	19.95	19.78	19.23	109	74	57	2
1.9	19.04	20.13	19.8	19.63	19.08	109	76	59	4
2	18.91	20	19.69	19.52	18.98	109	78	61	7

Table 5: Implied vol and its error for different methods, 10Y maturity, $\beta = 0.6$, $\rho = -0.5$.

	Value (%)					Difference (bps)			
K	MC	HL-P	Hagan	ZC Map	Hyb ZC Map	HL-P	Hagan	ZC Map	Hyb ZC Map
0.1	42.56	44.16	47.08	41.52	44.84	160	452	-104	228
0.2	36.81	38.1	40.19	36.18	38.54	129	338	-63	173
0.3	33.32	34.47	36.05	32.91	34.7	115	273	-41	138
0.4	30.81	31.87	33.09	30.55	31.92	106	228	-26	111
0.5	28.85	29.86	30.78	28.71	29.75	101	193	-14	90
0.6	27.27	28.24	28.91	27.22	27.98	97	164	-5	71
0.7	25.95	26.9	27.37	25.99	26.51	95	142	4	56
0.8	24.84	25.78	26.07	24.96	25.28	94	123	12	44
0.9	23.91	24.85	24.98	24.1	24.24	94	107	19	33
1	**23.13**	**24.07**	**24.07**	**23.38**	**23.38**	**94**	**94**	**25**	**25**
1.1	22.48	23.42	23.31	22.78	22.66	94	83	30	18
1.2	21.94	22.9	22.69	22.3	22.08	96	75	36	14
1.3	21.5	22.47	22.2	21.91	21.62	97	70	41	12
1.4	21.16	22.14	21.81	21.6	21.26	98	65	44	10
1.5	20.89	21.88	21.51	21.37	20.99	99	62	48	10
1.6	20.68	21.68	21.3	21.19	20.8	100	62	51	12
1.7	20.54	21.55	21.15	21.07	20.68	101	61	53	14
1.8	20.44	21.45	21.07	20.99	20.6	101	63	55	16
1.9	20.37	21.4	21.02	20.94	20.57	103	65	57	20
2	20.35	21.37	21.02	20.93	20.58	102	67	58	23

Table 6: Implied vol and its error for different methods, 10Y maturity, $\beta = 0.9$, $\rho = -0.5$.

	Value (%)					Difference (bps)			
K	MC	HL-P	Hagan	ZC Map	Hyb ZC Map	HL-P	Hagan	ZC Map	Hyb ZC Map
0.1	54.36	72.53	70.92	53.65	54.42	1817	1656	-71	6
0.2	45.77	56	56.02	45.21	45.83	1023	1025	-56	6
0.3	40.47	47.36	47.78	40.01	40.53	689	731	-46	6
0.4	36.62	41.67	42.17	36.24	36.68	505	555	-38	6
0.5	33.62	37.54	37.98	33.32	33.67	392	436	-30	5
0.6	31.2	34.36	34.71	30.96	31.24	316	351	-24	4
0.7	29.21	31.84	32.09	29.02	29.23	263	288	-19	2
0.8	27.55	29.81	29.96	27.41	27.55	226	241	-14	0
0.9	26.17	28.15	28.22	26.08	26.15	198	205	-9	-2
1	**25.02**	**26.8**	**26.8**	**24.98**	**24.98**	**178**	**178**	**-4**	**-4**
1.1	24.08	25.7	25.66	24.07	24.01	162	158	-1	-7
1.2	23.31	24.81	24.74	23.34	23.22	150	143	3	-9
1.3	22.69	24.1	24.03	22.76	22.58	141	134	7	-11
1.4	22.19	23.53	23.47	22.29	22.07	134	128	10	-12
1.5	21.8	23.08	23.05	21.93	21.67	128	125	13	-13
1.6	21.49	22.73	22.73	21.65	21.36	124	124	16	-13
1.7	21.26	22.47	22.49	21.44	21.13	121	123	18	-13
1.8	21.08	22.26	22.32	21.28	20.95	118	124	20	-13
1.9	20.94	22.11	22.21	21.16	20.82	117	127	22	-12
2	20.85	22	22.13	21.08	20.73	115	128	23	-12

Table 7: Implied vol and its error for different methods, 10Y maturity, $\beta = 0.3$, $\rho = -0.2$.

	Value (%)					Difference (bps)			
K	MC	HL-P	Hagan	ZC Map	Hyb ZC Map	HL-P	Hagan	ZC Map	Hyb ZC Map
0.1	48.5	55.39	56.52	47.84	49.03	689	802	-66	53
0.2	41.12	45.53	46.74	40.67	41.57	441	562	-45	45
0.3	36.72	40.03	41.06	36.39	37.11	331	434	-33	39
0.4	33.6	36.28	37.1	33.36	33.94	268	350	-24	34
0.5	31.23	33.5	34.13	31.06	31.51	227	290	-17	28
0.6	29.36	31.35	31.79	29.24	29.58	199	243	-12	22
0.7	27.85	29.64	29.94	27.78	28.03	179	209	-7	18
0.8	26.62	28.27	28.44	26.6	26.76	165	182	-2	14
0.9	25.64	27.18	27.25	25.66	25.73	154	161	2	9
1	**24.84**	**26.3**	**26.3**	**24.9**	**24.9**	**146**	**146**	**6**	**6**
1.1	24.22	25.61	25.57	24.31	24.25	139	135	9	3
1.2	23.73	25.08	25.01	23.85	23.73	135	128	12	0
1.3	23.35	24.67	24.59	23.51	23.34	132	124	16	-1
1.4	23.07	24.36	24.29	23.25	23.05	129	122	18	-2
1.5	22.87	24.13	24.09	23.07	22.85	126	122	20	-2
1.6	22.73	23.98	23.97	22.95	22.71	125	124	22	-2
1.7	22.64	23.87	23.9	22.88	22.62	123	126	24	-2
1.8	22.59	23.81	23.88	22.84	22.57	122	129	25	-2
1.9	22.57	23.79	23.9	22.83	22.56	122	133	26	-1
2	22.57	23.79	23.94	22.85	22.57	122	137	28	0

Table 8: Implied vol and its error for different methods, 10Y maturity, $\beta = 0.6$, $\rho = -0.2$.

	Value (%)					Difference (bps)			
K	MC	HL-P	Hagan	ZC Map	Hyb ZC Map	HL-P	Hagan	ZC Map	Hyb ZC Map
0.1	41.37	44.09	46.77	40.83	42.26	272	540	-54	89
0.2	35.89	37.99	39.87	35.54	36.61	210	398	-35	72
0.3	32.65	34.45	35.84	32.42	33.25	180	319	-23	60
0.4	30.39	32.02	33.04	30.24	30.9	163	265	-15	51
0.5	28.71	30.22	30.96	28.62	29.13	151	225	-9	42
0.6	27.42	28.84	29.36	27.38	27.76	142	194	-4	34
0.7	26.41	27.79	28.12	26.43	26.69	138	171	2	28
0.8	25.64	26.98	27.17	25.7	25.86	134	153	6	22
0.9	25.06	26.37	26.45	25.15	25.22	131	139	9	16
1	**24.63**	**25.93**	**25.93**	**24.76**	**24.76**	**130**	**130**	**13**	**13**
1.1	24.32	25.61	25.56	24.49	24.43	129	124	17	11
1.2	24.12	25.41	25.33	24.31	24.21	129	121	19	9
1.3	24.01	25.29	25.21	24.22	24.09	128	120	21	8
1.4	23.96	25.25	25.17	24.19	24.03	129	121	23	7
1.5	23.96	25.25	25.2	24.21	24.04	129	124	25	8
1.6	24.01	25.3	25.27	24.27	24.09	129	126	26	8
1.7	24.08	25.37	25.38	24.35	24.17	129	130	27	9
1.8	24.18	25.48	25.52	24.46	24.28	130	134	28	10
1.9	24.29	25.6	25.69	24.58	24.4	131	140	29	11
2	24.41	25.73	25.86	24.71	24.54	132	145	30	13

Table 9: Implied vol and its error for different methods, 10Y maturity, $\beta = 0.9$, $\rho = -0.2$.

	Value (%)					Difference (bps)			
K	MC	HL-P	Hagan	ZC Map	Hyb ZC Map	HL-P	Hagan	ZC Map	Hyb ZC Map
0.1	46.06	81.19	69.25	43.45	47.05	3513	2319	-261	99
0.2	39.55	59.5	55.07	37.41	40.16	1995	1552	-214	61
0.3	35.34	48.9	47.04	33.52	35.69	1356	1170	-182	35
0.4	32.13	42.12	41.38	30.57	32.28	999	925	-156	15
0.5	29.49	37.21	37.02	28.16	29.5	772	753	-133	1
0.6	27.23	33.4	33.46	26.12	27.13	617	623	-111	-10
0.7	25.24	30.3	30.45	24.34	25.05	506	521	-90	-19
0.8	23.46	27.7	27.85	22.75	23.21	424	439	-71	-25
0.9	21.85	25.48	25.57	21.34	21.56	363	372	-51	-29
1	**20.37**	**23.54**	**23.54**	**20.06**	**20.06**	**317**	**317**	**-31**	**-31**
1.1	19.02	21.84	21.72	18.9	18.7	282	270	-12	-32
1.2	17.79	20.34	20.08	17.86	17.47	255	229	7	-32
1.3	16.66	19.01	18.62	16.93	16.36	235	196	27	-30
1.4	15.63	17.86	17.32	16.1	15.37	223	169	47	-26
1.5	14.72	16.86	16.18	15.38	14.5	214	146	66	-22
1.6	13.92	16.02	15.2	14.76	13.75	210	128	84	-17
1.7	13.24	15.31	14.4	14.24	13.13	207	116	100	-11
1.8	12.67	14.74	13.75	13.82	12.63	207	108	115	-4
1.9	12.21	14.28	13.26	13.48	12.24	207	105	127	3
2	11.84	13.92	12.89	13.21	11.96	208	105	137	12

Table 10: Implied vol and its error for different methods, 20Y maturity, $\beta = 0.3$, $\rho = -0.8$.

	Value (%)					Difference (bps)			
K	MC	HL-P	Hagan	ZC Map	Hyb ZC Map	HL-P	Hagan	ZC Map	Hyb ZC Map
0.1	42.37	48.69	47	38.43	44.66	632	463	-394	229
0.2	36.28	40.15	40.26	33.48	37.84	387	398	-280	156
0.3	32.44	35.28	35.84	30.3	33.55	284	340	-214	111
0.4	29.58	31.85	32.51	27.89	30.34	227	293	-169	76
0.5	27.27	29.18	29.81	25.94	27.77	191	254	-133	50
0.6	25.32	27	27.53	24.28	25.61	168	221	-104	29
0.7	23.64	25.15	25.56	22.84	23.75	151	192	-80	11
0.8	22.14	23.54	23.82	21.56	22.12	140	168	-58	-2
0.9	20.8	22.12	22.26	20.41	20.67	132	146	-39	-13
1	**19.58**	**20.86**	**20.86**	**19.38**	**19.38**	**128**	**128**	**-20**	**-20**
1.1	18.48	19.73	19.58	18.45	18.22	125	110	-3	-26
1.2	17.47	18.72	18.43	17.6	17.19	125	96	13	-28
1.3	16.56	17.81	17.38	16.84	16.27	125	82	28	-29
1.4	15.73	17.01	16.45	16.16	15.45	128	72	43	-28
1.5	14.99	16.31	15.62	15.56	14.75	132	63	57	-24
1.6	14.33	15.69	14.9	15.03	14.15	136	57	70	-18
1.7	13.77	15.17	14.29	14.58	13.65	140	52	81	-12
1.8	13.29	14.72	13.79	14.19	13.24	143	50	90	-5
1.9	12.89	14.35	13.39	13.87	12.93	146	50	98	4
2	12.56	14.04	13.09	13.59	12.7	148	53	103	14

Table 11: Implied vol and its error for different methods, 20Y maturity, $\beta = 0.6$, $\rho = -0.8$.

	Value (%)					Difference (bps)			
K	MC	HL-P	Hagan	ZC Map	Hyb ZC Map	HL-P	Hagan	ZC Map	Hyb ZC Map
0.1	36.7	33.2	37.42	32.2	38.62	-350	72	-450	192
0.2	31.85	29.36	32.27	28.56	32.83	-249	42	-329	98
0.3	28.84	26.89	29.05	26.21	29.29	-195	21	-263	45
0.4	26.59	25.03	26.66	24.42	26.7	-156	7	-217	11
0.5	24.79	23.51	24.75	22.97	24.65	-128	-4	-182	-14
0.6	23.27	22.22	23.13	21.74	22.95	-105	-14	-153	-32
0.7	21.95	21.1	21.74	20.67	21.49	-85	-21	-128	-46
0.8	20.78	20.1	20.51	19.71	20.22	-68	-27	-107	-56
0.9	19.74	19.21	19.4	18.86	19.1	-53	-34	-88	-64
1	**18.8**	**18.41**	**18.41**	**18.1**	**18.1**	**-39**	**-39**	**-70**	**-70**
1.1	17.94	17.69	17.52	17.4	17.2	-25	-42	-54	-74
1.2	17.17	17.04	16.7	16.78	16.41	-13	-47	-39	-76
1.3	16.46	16.45	15.97	16.22	15.7	-1	-49	-24	-76
1.4	15.83	15.93	15.32	15.72	15.07	10	-51	-11	-76
1.5	15.26	15.46	14.74	15.27	14.53	20	-52	1	-73
1.6	14.77	15.05	14.24	14.88	14.06	28	-53	11	-71
1.7	14.33	14.7	13.8	14.54	13.67	37	-53	21	-66
1.8	13.95	14.38	13.44	14.24	13.35	43	-51	29	-60
1.9	13.64	14.11	13.15	13.98	13.1	47	-49	34	-54
2	13.38	13.88	12.92	13.75	12.91	50	-46	37	-47

Table 12: Implied vol and its error for different methods, 20Y maturity, $\beta = 0.9$, $\rho = -0.8$. The worst case for our approximation accuracy.

	Value (%)					Difference (bps)			
K	MC	HL-P	Hagan	ZC Map	Hyb ZC Map	HL-P	Hagan	ZC Map	Hyb ZC Map
0.1	45.51	81.23	76.03	42.66	45.32	3572	3052	-285	-19
0.2	39.09	60.57	59.73	36.67	38.81	2148	2064	-242	-28
0.3	34.99	50.35	50.78	32.9	34.66	1536	1579	-209	-33
0.4	31.92	43.8	44.63	30.1	31.56	1188	1271	-182	-36
0.5	29.45	39.09	39.97	27.88	29.07	964	1052	-157	-38
0.6	27.37	35.48	36.26	26.04	26.98	811	889	-133	-39
0.7	25.6	32.59	33.2	24.49	25.18	699	760	-111	-42
0.8	24.05	30.21	30.63	23.17	23.63	616	658	-88	-42
0.9	22.7	28.24	28.44	22.04	22.27	554	574	-66	-43
1	**21.52**	**26.58**	**26.58**	**21.08**	**21.08**	**506**	**506**	**-44**	**-44**
1.1	20.48	25.17	24.98	20.26	20.05	469	450	-22	-43
1.2	19.58	23.99	23.64	19.58	19.16	441	406	0	-42
1.3	18.81	23	22.51	19.01	18.4	419	370	20	-41
1.4	18.15	22.17	21.58	18.55	17.77	402	343	40	-38
1.5	17.6	21.49	20.83	18.17	17.25	389	323	57	-35
1.6	17.15	20.92	20.23	17.87	16.83	377	308	72	-32
1.7	16.78	20.46	19.76	17.63	16.5	368	298	85	-28
1.8	16.48	20.09	19.41	17.44	16.25	361	293	96	-23
1.9	16.24	19.78	19.14	17.29	16.06	354	290	105	-18
2	16.04	19.54	18.95	17.17	15.92	350	291	113	-12

Table 13: Implied vol and its error for different methods, 20Y maturity, $\beta = 0.3$, $\rho = -0.5$.

	Value (%)					Difference (bps)			
K	MC	HL-P	Hagan	ZC Map	Hyb ZC Map	HL-P	Hagan	ZC Map	Hyb ZC Map
0.1	41.89	53.36	55.22	38.24	42.7	1147	1333	-365	81
0.2	36.01	44.01	46.33	33.27	36.61	800	1032	-274	60
0.3	32.38	38.78	40.89	30.2	32.82	640	851	-218	44
0.4	29.72	35.18	36.97	27.96	30.03	546	725	-176	31
0.5	27.61	32.46	33.9	26.2	27.81	485	629	-141	20
0.6	25.88	30.29	31.4	24.76	25.98	441	552	-112	10
0.7	24.41	28.52	29.31	23.57	24.44	411	490	-84	3
0.8	23.16	27.04	27.54	22.57	23.11	388	438	-59	-5
0.9	22.08	25.79	26.03	21.72	21.98	371	395	-36	-10
1	**21.15**	**24.74**	**24.74**	**21.01**	**21.01**	**359**	**359**	**-14**	**-14**
1.1	20.35	23.85	23.64	20.42	20.19	350	329	7	-16
1.2	19.67	23.1	22.72	19.92	19.5	343	305	25	-17
1.3	19.09	22.47	21.96	19.52	18.93	338	287	43	-16
1.4	18.61	21.95	21.34	19.19	18.47	334	273	58	-14
1.5	18.21	21.52	20.84	18.92	18.1	331	263	71	-11
1.6	17.88	21.17	20.46	18.71	17.82	329	258	83	-6
1.7	17.62	20.88	20.17	18.55	17.61	326	255	93	-1
1.8	17.42	20.65	19.96	18.42	17.46	323	254	100	4
1.9	17.25	20.47	19.81	18.32	17.35	322	256	107	10
2	17.13	20.32	19.72	18.25	17.29	319	259	112	16

Table 14: Implied vol and its error for different methods, 20Y maturity, $\beta = 0.6$, $\rho = -0.5$.

	Value (%)					Difference (bps)			
K	MC	HL-P	Hagan	ZC Map	Hyb ZC Map	HL-P	Hagan	ZC Map	Hyb ZC Map
0.1	36.57	38.84	44.74	32.82	38.36	227	817	-375	179
0.2	31.92	34.13	38.33	29.25	33.26	221	641	-267	134
0.3	29.09	31.28	34.46	27.04	30.1	219	537	-205	101
0.4	27.04	29.23	31.67	25.43	27.8	219	463	-161	76
0.5	25.43	27.65	29.49	24.18	25.99	222	406	-125	56
0.6	24.12	26.37	27.73	23.18	24.51	225	361	-94	39
0.7	23.03	25.33	26.26	22.36	23.28	230	323	-67	25
0.8	22.1	24.46	25.04	21.68	22.25	236	294	-42	15
0.9	21.33	23.74	24	21.13	21.39	241	267	-20	6
1	**20.67**	**23.14**	**23.14**	**20.68**	**20.68**	**247**	**247**	**1**	**1**
1.1	20.12	22.64	22.42	20.32	20.1	252	230	20	-2
1.2	19.67	22.24	21.83	20.03	19.64	257	216	36	-3
1.3	19.3	21.91	21.36	19.8	19.27	261	206	50	-3
1.4	19	21.65	21	19.62	19	265	200	62	0
1.5	18.76	21.45	20.72	19.49	18.81	269	196	73	5
1.6	18.58	21.29	20.52	19.39	18.68	271	194	81	10
1.7	18.45	21.17	20.39	19.32	18.6	272	194	87	15
1.8	18.35	21.08	20.31	19.28	18.57	273	196	93	22
1.9	18.28	21.02	20.27	19.25	18.57	274	199	97	29
2	18.25	20.98	20.27	19.24	18.6	273	202	99	35

Table 15: Implied vol and its error for different methods, 20Y maturity, $\beta = 0.9$, $\rho = -0.5$.

	Value (%)					Difference (bps)			
K	MC	HL-P	Hagan	ZC Map	Hyb ZC Map	HL-P	Hagan	ZC Map	Hyb ZC Map
0.1	44.79	79.19	77.91	43.3	44.4	3440	3312	-149	-39
0.2	38.5	59.94	60.65	37.22	38.13	2144	2215	-128	-37
0.3	34.57	50.32	51.44	33.44	34.21	1575	1687	-113	-36
0.4	31.68	44.16	45.26	30.68	31.34	1248	1358	-100	-34
0.5	29.4	39.76	40.7	28.53	29.07	1036	1130	-87	-33
0.6	27.54	36.43	37.14	26.79	27.22	889	960	-75	-32
0.7	25.99	33.81	34.3	25.35	25.68	782	831	-64	-31
0.8	24.69	31.71	32	24.17	24.39	702	731	-52	-30
0.9	23.6	30	30.13	23.19	23.29	640	653	-41	-31
1	**22.68**	**28.6**	**28.6**	**22.38**	**22.38**	**592**	**592**	**-30**	**-30**
1.1	21.93	27.46	27.37	21.72	21.62	553	544	-21	-31
1.2	21.3	26.52	26.39	21.2	21	522	509	-10	-30
1.3	20.79	25.76	25.62	20.78	20.49	497	483	-1	-30
1.4	20.37	25.14	25.02	20.45	20.09	477	465	8	-28
1.5	20.04	24.63	24.56	20.19	19.77	459	452	15	-27
1.6	19.78	24.22	24.22	19.99	19.52	444	444	21	-26
1.7	19.58	23.9	23.96	19.84	19.33	432	438	26	-25
1.8	19.42	23.64	23.78	19.73	19.19	422	436	31	-23
1.9	19.3	23.43	23.65	19.65	19.08	413	435	35	-22
2	19.2	23.26	23.57	19.6	19.01	406	437	40	-19

Table 16: Implied vol and its error for different methods, 20Y maturity, $\beta = 0.3$, $\rho = -0.2$.

	Value (%)					Difference (bps)			
K	MC	HL-P	Hagan	ZC Map	Hyb ZC Map	HL-P	Hagan	ZC Map	Hyb ZC Map
0.1	41.26	56.03	58.97	39.55	41.35	1477	1771	-171	9
0.2	35.62	46.2	48.86	34.29	35.68	1058	1324	-133	6
0.3	32.21	40.81	42.96	31.11	32.24	860	1075	-110	3
0.4	29.76	37.17	38.85	28.85	29.77	741	909	-91	1
0.5	27.88	34.49	35.75	27.13	27.86	661	787	-75	-2
0.6	26.39	32.43	33.33	25.78	26.34	604	694	-61	-5
0.7	25.17	30.8	31.39	24.69	25.1	563	622	-48	-7
0.8	24.19	29.5	29.84	23.83	24.08	531	565	-36	-11
0.9	23.38	28.45	28.59	23.13	23.26	507	521	-25	-12
1	**22.74**	**27.61**	**27.61**	**22.59**	**22.59**	**487**	**487**	**-15**	**-15**
1.1	22.22	26.93	26.84	22.17	22.06	471	462	-5	-16
1.2	21.81	26.4	26.26	21.85	21.65	459	445	4	-16
1.3	21.5	25.98	25.83	21.61	21.34	448	433	11	-16
1.4	21.26	25.65	25.52	21.44	21.11	439	426	18	-15
1.5	21.08	25.39	25.31	21.32	20.94	431	423	24	-14
1.6	20.96	25.2	25.18	21.24	20.83	424	422	28	-13
1.7	20.87	25.06	25.12	21.2	20.77	419	425	33	-10
1.8	20.82	24.96	25.1	21.18	20.73	414	428	36	-9
1.9	20.79	24.89	25.12	21.19	20.73	410	433	40	-6
2	20.79	24.85	25.17	21.21	20.74	406	438	42	-5

Table 17: Implied vol and its error for different methods, 20Y maturity, $\beta = 0.6$, $\rho = -0.2$.

	Value (%)					Difference (bps)			
K	MC	HL-P	Hagan	ZC Map	Hyb ZC Map	HL-P	Hagan	ZC Map	Hyb ZC Map
0.1	36.27	42.87	48.26	34.62	36.9	660	1199	-165	63
0.2	31.85	37.41	41.19	30.62	32.35	556	934	-123	50
0.3	29.23	34.27	37.05	28.25	29.62	504	782	-98	39
0.4	27.39	32.12	34.18	26.61	27.69	473	679	-78	30
0.5	26.01	30.54	32.03	25.39	26.23	453	602	-62	22
0.6	24.95	29.35	30.38	24.47	25.1	440	543	-48	15
0.7	24.13	28.44	29.11	23.78	24.22	431	498	-35	9
0.8	23.5	27.75	28.13	23.26	23.53	425	463	-24	3
0.9	23.02	27.23	27.39	22.88	23.01	421	437	-14	-1
1	**22.66**	**26.85**	**26.85**	**22.62**	**22.62**	**419**	**419**	**-4**	**-4**
1.1	22.41	26.58	26.48	22.45	22.35	417	407	4	-6
1.2	22.24	26.4	26.25	22.35	22.18	416	401	11	-6
1.3	22.14	26.29	26.12	22.31	22.08	415	398	17	-6
1.4	22.09	26.23	26.08	22.32	22.04	414	399	23	-5
1.5	22.09	26.22	26.11	22.35	22.06	413	402	26	-3
1.6	22.12	26.24	26.19	22.41	22.1	412	407	29	-2
1.7	22.17	26.29	26.31	22.49	22.18	412	414	32	1
1.8	22.24	26.36	26.46	22.59	22.28	412	422	35	4
1.9	22.33	26.45	26.63	22.69	22.39	412	430	36	6
2	22.42	26.55	26.81	22.81	22.51	413	439	39	9

Table 18: Implied vol and its error for different methods, 20Y maturity, $\beta = 0.9$, $\rho = -0.2$.

For better visualization, we present two graphs for correlations $\rho = -0.5$ and skew $\beta = 0.6$.

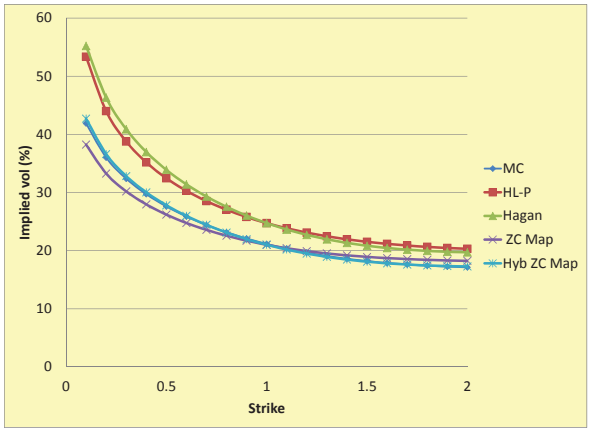

Figure 1: Implied volatilities: maturity 20Y.

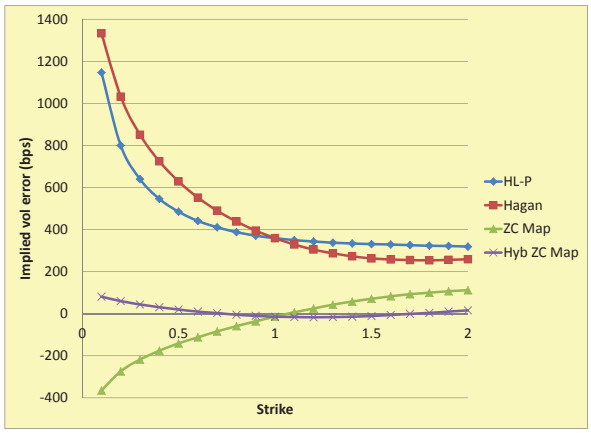

Figure 2: Implied volatility errors w.r.t. MC: maturity 20Y.

Given presented results, we observe an excellent approximation quality for small and moderate correlation for the Maps to the SABR ZC, their slight degeneration for large correlation, and insufficient approximation accuracy for Hagan or Henry-Labordere&Paulot methods for large maturities >10Y. We see that Hybrid ZC Map can deliver slightly better overall fit for large maturities that the regular ZC Map.

In the table below, we summarize results for the centered second moment $E[(F_T - F_0)^2]$ calculated for correlations $\rho = -0.5$ and skew $\beta = 0.6$.

	Values		Errors w.r.t. MC	
Maturity	10Y	20Y	10Y	20Y
MC	0.7639	1.025		
HL-P	0.8162	1.255	0.0523	0.23
Hagan	0.8263	1.733	0.0624	0.708
ZC Map	0.7817	1.065	0.0178	0.04
Hyb ZC Map	0.7826	1.194	0.0187	0.169

Table 19: Centered second moment and its errors for different methods.

The second-moment table demonstrates an excellent approximation quality for the regular SABR ZC Map and insufficient accuracy for the Hagan method, Henry-Labordere&Paulot one as well as the Hybrid ZC Map for large maturities. To understand a reason for this non-accurate behavior of the Hybrid ZC Map we recall that its first order correction corresponds to the ATM strike. For large maturities the second moment integration (7.1) can go quite far in strikes[11] which leads to significant error accumulation for this non-optimal first order correction. The same picture can be observed for the Hagan method compared with Henry-Labordere&Paulot one where the Hagan first order and corrections are sub-optimal for extreme strikes.

Thus, we can recommend the Hybrid ZC Map for close to ATM option pricing for large maturities due to its simplicity. However, more complicated regular SABR ZC Map can be used for both option pricing and second moment replication for any maturities.

8 Conclusion

We presented an exact formula for option prices for the zero correlation SABR model which involves a 2D integration over an elementary function permitting an efficient numerical implementation. We applied an efficient expansion map for option prices for non-zero correlation SABR, delivering excellent approximation quality for small/moderate correlations. Approximation simplicity permits a straightforward implementation.

[11] For example, in the setup above the option price reaches 10^{-6} for strikes around 35.

We have checked the accuracy for the option pricing itself and the second moment underlying the CMS payment pricing.

The authors are indebted to Serguei Mechkov for discussions and numerical implementation help as well as to their colleagues at Numerix, especially to Gregory Whitten and Serguei Issakov for supporting this work and Patti Harris for the excellent editing. We are grateful to Michael Konikov and Alexander Lipton for stimulating discussions.

References

[1] Andreasen J. and Huge B. (2011). "No arbitarge SABR", ICBI Global Derivatives Presentation.

[2] Antonov A. and Misirpashaev T. (2009). "Projection on a Quadratic Model by Asymptotic Expansion with an Application to LMM Swaption", SSRN paper.

[3] Antonov A. and Spector M. (2011). "Advanced analytics for the SABR model", WBS 7th Fixed Income Conference Presentation.

[4] Avramidi I. (2007). "Analytic and Geometric Methods for Heat Kernel Applications in Finance", `http://infohost.nmt.edu/~iavramid/notes/hkt/hktslides7b.pdf`.

[5] Berestycki H., Busca J., and Florent I. (2004). "Computing the implied volatility in stochastic volatility models", Communications on Pure and Applied Mathematics, 57(10), 1352–1373.

[6] Carr P. and Schroder M. (2004). "Bessel processes, the integral of geometric brownian motion, and asian options", Theory Probab. Appl. V. 48, 400–425.

[7] DeWitt B. (1965). "Dynamical Theory of Groups and Fields", Gordon and Breach.

[8] Hagan P., Kumar D., Lesnievski A., and Woodward D. (2002). "Managing Smile Risk", Wilmott Magazine, v.3, 84–108.

[9] Hagan P. (2003). "Convexity Conundrums: Pricing CMS Swaps, Caps, and Floors", Wilmott magazine, March, 38–44.

[10] Henry-Labordere P. (2008). "Analysis, Geometry, and Modeling in Finance: Advanced Methods in Option Pricing", Chapman & Hall.

[11] Islah O. (2009). "Solving SABR in exact form and unifying it with LIBOR market model", SSRN paper.

[12] Jeanblanc M., Yor M., and Chesney M. (2009). Mathematics Methods for Financial Markets, Springer.

[13] Lipton A. and Sepp A. (2011). "Credit value adjustment in the extended strutural default model", Chapter 12 in "The Oxford Handbook of Credit Derivatives", A. Lipton and A. Rennie, eds., Oxford University Press.

[14] McKean H.P.(1970). "An upper bound to the spectrum of Δ on a manifold of negative curvature", J. Diff. Geom., 4, 359–366.

[15] Mercurio F. and Moreni N. (2009). "Inflation modelling with SABR dynamics", Risk June, 106–111.

[16] Mercurio F. and Morini M. (2009). "Joining the SABR and Libor models together", Risk March, 80–85.

[17] Obloj J. (2008). "Fine-tune your smile: Correction to Hagan et al", Wilmott Magazine, May.

[18] Paulot L. (2009). "Asymptotic Implied Volatility at the Second Order with Application to the SABR Model", SSRN paper.

[19] Rebonato R., McKay K. and White R. (2009). "The SABR/LIBOR Market Model: Pricing, Calibration and Hedging for Complex Interest-Rate Derivatives", John Wiley & Sons Ltd.

[20] Yor M. (1992). "On Some Exponential Functionals of Brownian Motion" Advances in Applied Probability, 24(3), 509.

A Joint distribution of a geometric Brownian motion and its integral

Let process

$$X_t^{(\nu)} = x_0 e^{2\nu t + 2W_t}$$

be exponential of Brownian motion with drift 2ν driven by the SDE

$$dX_t = 2(\nu+1)X_t\ dt + 2X_t\ dW_t, \tag{A.1}$$

and let

$$A_t^{(\nu)} = \int_0^t X_{t'}^{(\nu)} dt' \tag{A.2}$$

be its integral accumulated up to moment t. The joint distribution of $X_t^{(\nu)}$ and $A_t^{(\nu)}$ is defined as

$$p(t,\tau,x \mid x_0) = \mathbb{E}_{\{W\}}\left\{\delta\left(X_t^{(\nu)} - x\right)\ \delta\left(A_t^{(\nu)} - \tau\right) \mid x_0\right\}$$

and the main difficulty in finding it is the path dependence of integral $A_t^{(\nu)}$. However, the following key steps allow us to resolve the problem.

First, we apply the Laplace transform (LT) in time t by changing of the order of integration and averaging. Then, we switch to the stochastic time $\tau = A_t^{(\nu)}$ and make use of the Lamperti

property of a Geometric Brownian motion (GBM). Recall that it states that a GBM $X_t^{(\nu)}$ is a time-changed (squared) Bessel process $Y_\tau^{(\nu)}$ with index ν in a new stochastic time $\tau = A_t^{(\nu)}$

$$X_t^{(\nu)} = Y_{A_t}^{(\nu)}.$$

Effective path dependence in the desired PDF is bypassed onto Laplacian factor $\exp\{-\lambda t_0\}$ with original time becoming a non-local functional, $t_0 = \int_0^\tau d\tau'/Y_{\tau'}$. Remarkably, the non-locality can be eliminated by the simple drift shift with changes of the Brownian measure according to Girsanov theorem. As a result, the LT of the joint PDF is proved to be proportional to the probability density of the squared Bessel process with shifted index $\mu = (\nu^2 + 2\lambda)^{1/2}$ depending on the Laplace parameter λ. Finally, the inverse LT restores dependence on the original time t.

Now we pass to the detailed derivation. First, we describe the Lamperti property of a GBM $X_t^{(\nu)}$. Denote by $Y_\tau^{(\nu)}$ the process $X_t^{(\nu)}$ measured in stretched time $\tau = A_t^{(\nu)}$,

$$\begin{aligned} Y_{A_t}^{(\nu)} &\equiv X_t^{(\nu)} \\ d\tau &= X_t^{(\nu)}\, dt \end{aligned}$$

and let an SDE for $Y_\tau^{(\nu)}$ be

$$dY_\tau^{(\nu)} = a\, d\tau + b\, dB_\tau.$$

Comparing it with the SDE (A.1), we get the drift coefficient

$$a = 2(\nu + 1)$$

equating the drift terms. Next, from the stochastic terms equality, $b\ dB_\tau = 2X_t^{(\nu)}\ dW_t$, we obtain

$$b^2 d\tau = 4{X_t^{(\nu)}}^2 dt$$

or

$$b = 2\sqrt{X_t^{(\nu)}} = 2\sqrt{Y_\tau^{(\nu)}}.$$

Thus, the resulting SDE for the process $Y_\tau^{(\nu)}$

$$dY_\tau = 2(\nu + 1)d\tau + 2\sqrt{Y_\tau}\ dB_\tau$$

proves that $Y_\tau^{(\nu)}$ coincides with a squared Bessel process with index μ.

The Brownian motion B_τ adapted to the new time τ is defined in terms of original processes as

$$dB_\tau = \frac{2X_t^{(\nu)}\ dW_t}{b} = \sqrt{X_t^{(\nu)}}\ dW_t.$$

The new Brownian measure coincides with the original one because

$$-\frac{1}{2}\frac{(dB_{1\tau})^2}{d\tau} = -\frac{1}{2}\left(\frac{dW_{1t}}{dt}\right)^2 dt.$$

Next, we apply the Laplace transform (LT) and place the expectation operator outside the integral over time

$$\begin{aligned}\hat{p}(\lambda,\tau,x \mid x_0) &= \int_0^\infty dt\ e^{-\lambda t}\ p(t,\tau,x \mid x_0\ ) \\ &= \mathbb{E}_{\{W\}}\left\{\int_0^\infty dt\ e^{-\lambda t}\ \delta(X_t - x)\ \delta(A_t - \tau)\ \right\}. \end{aligned} \tag{A.3}$$

The integral over t is calculated with the help of τ- delta function. For a given τ, let t_0 be a moment such that $A_{t_0} = \tau$. Then

$$\delta(A_t - \tau) = \frac{1}{A'_{t_0}}\delta(t - t_0) = \frac{1}{X^{(\nu)}_{t_0}}\delta(t - t_0),$$

and the LT becomes

$$\hat{p}(\lambda,\tau,x \mid x_0) = \frac{1}{x}\mathbb{E}_{\{W\}}\left\{e^{-\lambda t_0}\ \delta(X^{(\nu)}_{t_0} - x)\right\} \tag{A.4}$$

where $t_0 = A^{-1}(\tau)$ is a stochastic path dependent process.

Next, it proves technically simpler to change measures for the original Brownian motion W_t, introducing a new Brownian motion $\tilde{W}_t$

$$W_t = \tilde{W}_t + \kappa t$$

for some shift κ which will be defined later. The process $X^{(\nu)}_t$ in the new measure has a changed drift, $\tilde{\nu} = \nu + \kappa$,

$$X^{(\nu+\kappa)}_t = x_0 e^{2(\nu+\kappa)t + 2\tilde{W}_t}. \tag{A.5}$$

The original and new Brownian measures are related as follows (Girsanov)

$$\mathbb{P}_{\{W\}} = \mathbb{P}_{\{\tilde{W}\}} e^{-\kappa\tilde{W}_t - \frac{\kappa^2 t}{2}}.$$

For the GBM (A.5), the factor $\exp(-\kappa\tilde{W}_t)$ can be expressed through the new GBM and the time

$$e^{-\kappa\tilde{W}_t} = \left(\frac{X^{(\nu+\kappa)}_t}{X_0}\right)^{-\kappa/2} e^{\kappa(\kappa+\nu)t}$$

and the Girsanov relation can be rewritten as

$$\mathbb{P}_{\{W\}} = \mathbb{P}_{\{\tilde{W}\}} \left(\frac{X_t^{(\nu+\kappa)}}{x_0} \right)^{-\kappa/2} e^{\frac{1}{2}\kappa(\kappa+2\nu)t}.$$

Applying this change of measure to the LT (A.4) at $t = t_0$, we get

$$\hat{p}(\lambda, \tau, x \mid x_0) = \frac{1}{x} \left(\frac{x}{x_0} \right)^{-\kappa/2} \mathbb{E}_{\{\tilde{W}\}} \left\{ e^{\frac{1}{2}(\kappa^2+2\kappa\nu-2\lambda)t_0} \; \delta(X_{t_0}^{(\nu+\kappa)} - x) \right\}.$$

Now choose κ to be a root of the quadratic polynomial $\kappa^2 + 2\kappa\nu - 2\lambda$ in the exponent above,

$$\kappa = -\nu + \sqrt{\nu^2 + 2\lambda},$$

thus eliminating the non-local exponential altogether. Denote

$$\mu = \left(\nu^2 + 2\lambda\right)^{1/2} \tag{A.6}$$

and define μ as the branch of the square root with positive real part, $\operatorname{Re}\mu > 0$ at $\operatorname{Re}\lambda > 0$. Note also that the changed drift becomes $\tilde{\nu} = \nu + \kappa = \mu$, and the LT of the joint PDF simplifies to

$$\hat{p}(\lambda, \tau, x \mid x_0) = \frac{1}{x} \left(\frac{x}{x_0} \right)^{-\frac{\mu-\nu}{2}} \mathbb{E}_{\{\tilde{W}\}} \left\{ \delta(X_{t_0}^{(\mu)} - x) \right\}.$$

Now we switch to the time τ and, using the Lamperti property $\mathbb{E}_{\{\tilde{W}_t\}} = \mathbb{E}_{\{B_\tau\}}$ and $X_{t_0}^{(\mu)} \equiv Y_{A_{t_0}}^{(\mu)} = Y_\tau^{(\mu)}$, obtain

$$\hat{p}(\lambda, \tau, x \mid x_0) = \frac{1}{x} \left(\frac{x}{x_0} \right)^{-\frac{\mu-\nu}{2}} \mathbb{E}_{\{B\}} \left\{ \delta(Y_\tau^{(\mu)} - x) \right\}.$$

The expectation is nothing but the PDF of the squared Bessel process $Y_\tau^{(\mu)}$

$$\mathbb{E}_{\{B\}} \left\{ \delta(Y_\tau^{(\mu)} - x) \right\} = \frac{1}{2\tau} \left(\frac{x}{x_0} \right)^{\frac{\mu}{2}} e^{-\frac{x+x_0}{2\tau}} I_\mu\left(\frac{\sqrt{xx_0}}{\tau}\right)$$

resulting in

$$\hat{p}(\lambda, \tau, x \mid x_0) = \frac{1}{2\tau x} \left(\frac{x}{x_0} \right)^{\frac{\nu}{2}} e^{-\frac{x+x_0}{2\tau}} I_\mu\left(\frac{\sqrt{xx_0}}{\tau}\right). \tag{A.7}$$

Notice that dependence on the Laplace parameter λ is solely through index μ of the Bessel function.

Finally, we take the inverse Laplace transform

$$p(t,\tau,x \mid x_0) = \frac{1}{2\pi i}\int_{C_B} \hat{p}(\lambda,\tau,x \mid x_0)e^{\lambda t}d\lambda$$

where contour C_B is a standard Bromwich contour in the complex plane λ, i.e., a vertical line $\operatorname{Re}\lambda = const > 0$. We take parameter μ defined by (A.6) as a new variable, then expressing $\lambda = \frac{1}{2}(\mu^2 - \nu^2)$ and using expression (A.7) for $\hat{p}$, we come up with

$$p(t,\tau,x \mid x_0) = \left(\frac{x}{x_0}\right)^{\frac{\nu}{2}} e^{-\frac{1}{2}\nu^2 t}\frac{1}{2\tau x}e^{-\frac{x+x_0}{2\tau}}\vartheta\left(\frac{\sqrt{xx_0}}{\tau},t\right) \tag{A.8}$$

where $\vartheta(r,t)$ is the Yor function defined as

$$\vartheta(r,t) = \frac{1}{2\pi i}\int_{C_\mu} I_\mu(r)\; e^{\frac{1}{2}\mu^2 t}\;\mu d\mu. \tag{A.9}$$

Contour C_μ in the complex plane μ is the image of a vertical line $\operatorname{Re}\lambda = const > 0$ and represents the right branch ($\operatorname{Re}\mu > |\nu|$) of a hyperbola with asymptotic directions $\frac{\operatorname{Im}\mu}{\operatorname{Re}\mu} = \pm 1$, indeed

$$(\operatorname{Re}\mu)^2 - (\operatorname{Im}\mu)^2 = \operatorname{Re}(\mu^2) = \nu^2 + 2\operatorname{Re}\lambda = const > \nu^2.$$

Use now an integral representation for the modified Bessel function $I_\mu(r)$

$$I_\mu(r) = \int_{C_w} e^{r\cosh w - \mu w}\;\frac{dw}{2\pi i} \tag{A.10}$$

where contour C_w consists of three legs: the first one running horizontally to the left from $(+\infty - i\pi)$ to $(0 - i\pi)$, the second one running vertically from $(0 - i\pi)$ to $(0 + i\pi)$, and the third leg running horizontally to the right from $(0 + i\pi)$ to $(+\infty + i\pi)$.

Then, we change the order of integration and represent function $\vartheta(r,t)$ as a double integral

$$\vartheta(r,t) = \int_{C_w} e^{r\cosh w}\;\frac{dw}{2\pi i}\int_{C_\mu} e^{\frac{1}{2}\mu^2 t - \mu w}\;\frac{\mu d\mu}{2\pi i}.$$

We manipulate it slightly representing $\mu e^{-\mu w} = -\frac{\partial}{\partial w}e^{-\mu w}$ and integrating by parts over w,

$$\vartheta(r,t) = r\int_{C_w} e^{r\cosh w}\;\sinh w\frac{dw}{2\pi i}\int_{C_\mu} e^{\frac{1}{2}\mu^2 t - \mu w}\;\frac{d\mu}{2\pi i}.$$

Without changing the value of μ-integral, we can straighten hyperbola C_μ to convert it into a vertical line. Indeed, the integrand is an analytical function and the crucial exponent decays: $\exp(\mu^2 t/2)$ at $\mu = R\,e^{i\varphi}$ with large R and $\pi/4 < |\varphi| < \pi/2$ so that $\operatorname{Re}(\mu^2) = R^2\cos 2\varphi < 0$.

The integral over μ becomes Gaussian after completing the square $\frac{1}{2}\mu^2 t - \mu w = \frac{t}{2}(\mu - w/t)^2 - \frac{w^2}{2t}$ and shifting $\mu = w/t + i\eta$ with real η, thus resulting in

$$\vartheta(r,t) = \frac{r}{2\pi i\sqrt{2\pi t}} \int_{C_w} e^{r\cosh w - \frac{w^2}{2t}} \sinh w \; dw.$$

Now consider the three legs of contour C_w. On the first leg, $w = \mathrm{Re}\, w - i\pi$, and we make the substitution $w = -\xi - i\pi$ with (real) ξ running from $(-\infty)$ to 0. On the third leg, $w = \mathrm{Re}\, w + i\pi$, and we make substitution $w = \xi + i\pi$ with ξ running now from 0 to $(+\infty)$. In both cases, $w^2 = (\xi + i\pi)^2$, $\cosh w = -\cosh\xi$, and $\sinh w \; dw = d(\cosh w) = -d(\cosh\xi) = -\sinh\xi \; d\xi$. Integrands are the same, and limits complement one another to the full real axis. The contribution from the second leg ($w = i\varphi$) is zero because the integrand is an odd function of φ (due to $\sinh w = i\sin\varphi$) while the limits of integration ($\pm\pi$) are symmetrical. As a result, we find a considerably compact form for $\vartheta(r,t)$,

$$\vartheta(r,t) = \frac{r}{-2\pi i\sqrt{2\pi t}} \int_{-\infty}^{+\infty} e^{-r\cosh\xi - \frac{(\xi+i\pi)^2}{2t}} \sinh\xi d\xi. \tag{A.11}$$

The result of the integration is real due to the even-odd properties of the integrand. Indeed, rewriting the exponent,

$$e^{-\frac{(\xi+i\pi)^2}{2t}} = e^{-\frac{\xi^2-\pi^2}{2t}} \left(\cos\frac{\pi\xi}{t} - i\sin\frac{\pi\xi}{t}\right),$$

we see that only the term with the odd factor $\sin\frac{\pi\xi}{t}$ contributes due to presence of another odd function $\sinh\xi$. This permits us to recast the function $\vartheta(r,t)$ into its usual form (Yor (1992))

$$\vartheta(r,t) = \frac{re^{\frac{\pi^2}{2t}}}{\pi\sqrt{2\pi t}} \int_0^{+\infty} e^{-r\cosh\xi - \frac{\xi^2}{2t}} \sinh\xi \sin\frac{\pi\xi}{t} d\xi. \tag{A.12}$$

B Details of option pricing derivation for zero correlation

B.1 Integrating with payoff

Following the plan sketched in Section 4.2, we rewrite probability density (4.12) as the PDF for the rate F,

$$\begin{aligned} p\left(t, F \mid F_0\right) &= \int_0^\infty dV \; p\left(t, F, V \mid F_0, V_0\right) \\ &= e^{-t/8} \int_0^\infty \frac{2dV}{V} \left(\frac{V}{V_0}\right)^{-1/2} \int_0^\infty d\tau \; p^{(\nu)}(\tau, F \mid F_0) \; \frac{e^{-\frac{V^2+V_0^2}{2\tau}}}{2\tau} \vartheta\left(\frac{VV_0}{\tau}, t\right). \end{aligned} \tag{B.1}$$

Recall here our PDF notation convention. The PDF of the SABR rate F_t is denoted using *argument* F, that is, $p^{(\nu)}(t, F \mid F_0) = E[\delta(F_t - F)]$, while we write the PDF of the corresponding *Bessel* process $Q_t = \frac{F_t^{1-\beta}}{1-\beta}$ using semantically the same function $p^{(\nu)}(t, q \mid q_0) = E[\delta(Q_t - q)]$, but with the *argument* q.

Now, we collect factors depending on τ and integrate by parts to generate the τ derivative of $p^{(\nu)}(\tau, F)$ (additional factor $1/\tau$ in the first line below originates from $r = \frac{VV_0}{\tau}$in $\vartheta\,(r, t)$ (A.12))

$$\begin{aligned}\int_0^\infty p^{(\nu)}(\tau, F \mid F_0)\; e^{-\frac{A}{2\tau}} \frac{d\tau}{2\tau^2} &= -\frac{1}{A}\int_0^\infty p^{(\nu)}(\tau, F \mid F_0)\; d_\tau \left(1 - e^{-\frac{A}{2\tau}}\right) \\ &= \frac{1}{A} p^{(\nu)}(0, F \mid F_0) + \frac{1}{A}\int_0^\infty d\tau \;\left[\partial_\tau p^{(\nu)}(\tau, F \mid F_0)\right]\;\left(1 - e^{-\frac{A}{2\tau}}\right)\end{aligned}$$

where

$$A = V^2 + V_0^2 + 2VV_0 \cosh\xi\ .$$

Then, we substitute the result into (B.1). The first part of the expression containing $p^{(\nu)}(0, F \mid F_0)$, can be simplified to $\delta(F - F_0) = p^{(\nu)}(0, F \mid F_0)$. Indeed, the integral $(B.1)$ with the PDF $p^{(\nu)}(\tau, F \mid F_0)$ replaced by one will be equal to one as far as it will represent integrated density of the joint distribution function of the stochastic time and the stochastic volatility. Thus,

$$\begin{aligned}p\,(t, F \mid F_0) - \delta(F - F_0) = \frac{e^{-t/8}}{-2\pi i\sqrt{2\pi t}} \int_0^\infty d\tau \;\left[\tfrac{1}{2}\partial_{FF}^2 F^{2\beta} p^{(\nu)}(\tau, F \mid F_0)\right] \\ \int_0^\infty \frac{2dV}{V}\left(\frac{V}{V_0}\right)^{-1/2} \int_{-\infty}^\infty d\xi \sinh\xi\;\frac{VV_0}{A}\left(1 - e^{-\frac{A}{2\tau}}\right) e^{-\frac{(\xi + i\pi)^2}{2t}}.\end{aligned} \tag{B.2}$$

Now we can easily integrate this expression with the call option payoff $(F - K)^+$ to get the option value, i.e.,

$$\int_0^\infty dF\;(F - K)^+ \frac{1}{2}\partial_F^2 \left(F^{2\beta} p(\tau, F \mid F_0)\right) = \frac{1}{2}\,K^{2\beta}\,p^{(\nu)}\,(\tau, K \mid F_0))\,. \tag{B.3}$$

It is further convenient to pass to the PDF of the associated BESQ process $X_t = \frac{F_t^{2(1-\beta)}}{(1-\beta)^2}$, which we denote as $p^{(-|\nu|)}(\tau, x \mid x_0)$ according to our argument conventions,

$$\frac{1}{2}\,K^{2\beta} p^{(\nu)}\,(\tau, K \mid F_0)) = 2|\nu| K\;p^{(-|\nu|)}(\tau, x_K \mid x_0) \tag{B.4}$$

with x_K and x_0 defined as

$$x_K = \frac{K^{2(1-\beta)}}{(1-\beta)^2} \quad \text{and} \quad x_0 = \frac{F_0^{2(1-\beta)}}{(1-\beta)^2}$$

and

$$p^{(-|\nu|)}(\tau, x \mid x_0) = \frac{e^{-\frac{x+x_0}{2\tau}}}{2\tau} \left(\frac{x}{x_0}\right)^{-|\nu|/2} I_{|\nu|}\left(\frac{\sqrt{xx_0}}{\tau}\right).$$

Using these results, we obtain the option time value as a three dimensional integral

$$C(t,K,F_0) - (F_0-K)^+ = 2|\nu|K \, \frac{e^{-t/8}}{(-2\pi i)\sqrt{2\pi t}} \int_0^\infty d\tau \; p^{(-|\nu|)}(\tau, x_K \mid x_0)$$
$$\int_0^\infty \frac{dV}{V} \left(\frac{V}{V_0}\right)^{-1/2} \int_{-\infty}^\infty \sinh\xi \; d\xi \frac{2VV_0}{A} \left(1 - e^{-\frac{A}{2\tau}}\right) e^{-\frac{(\xi+i\pi)^2}{2t}}. \quad \text{(B.5)}$$

B.2 Integrating stretched time out

Collect τ-dependent factors in the option price integral (B.5)

$$J_{(\tau)} = \int_0^\infty d\tau \; p^{(-|\nu|)}(\tau, x_K \mid x_0) \; \left(1 - e^{-\frac{A}{2\tau}}\right)$$
$$= \left(\frac{x_K}{x_0}\right)^{-|\nu|/2} \int_0^\infty \frac{d\tau}{2\tau} \; e^{-\frac{x_K+x_0}{2\tau}} I_{|\nu|}(\tfrac{\sqrt{x_K x_0}}{\tau}) \; \left(1 - e^{-\frac{A}{2\tau}}\right).$$

Throughout the appendix, we will refer to certain integrals as we do above for $J_{(\tau)}$, using the subscript to denote the integration variable.

Now set $s = \frac{\sqrt{x_K x_0}}{\tau}$ as the integration variable and adopt the following notations

$$b = \tfrac{x_K+x_0}{2\sqrt{x_K x_0}} > 1, \quad \text{(B.6)}$$

$$a = b + \tfrac{A}{2\sqrt{x_K x_0}} \equiv b + \frac{V^2 + V_0^2 + 2VV_0\cosh\xi}{2\sqrt{x_K x_0}} > b. \quad \text{(B.7)}$$

Then the above integral can be rewritten as

$$J_{(\tau)} = \left(\frac{x_K}{x_0}\right)^{-|\nu|/2} \int_0^\infty \frac{ds}{2s} \; I_{|\nu|}(s) \; \left(e^{-bs} - e^{-as}\right) = \tfrac{1}{2} \left(\frac{x_K}{x_0}\right)^{-|\nu|/2} \left[J_{(s)}(b) - J_{(s)}(a)\right] \quad \text{(B.8)}$$

where $J_{(s)}(b)$ is the Lipschitz-Hankel integral

$$J_{(s)}(b) = \int_0^\infty \frac{ds}{s} \; e^{-bs} I_{|\nu|}(s) \; = \frac{e^{-|\nu| \;\; \operatorname{arccosh} b}}{|\nu|}.$$

We give the derivation of this formula since we need an intermediate result. Regarding convergence of the integral, we notice that at large s function $I_{|\nu|}(s) \sim e^s$, and convergence is guaranteed by $b > 1$. At small s, the Bessel function $I_{|\nu|}(s)$ behaves like $I_{|\nu|}(s) \sim s^{|\nu|}$, which is sufficient for

convergence at zero. However, this behavior is hidden when we use an integral representation for $I_{|\nu|}(s)$. Therefore, we strengthen convergence by inserting factor s^{ε}, and take in the end limit of $\varepsilon \to +0$

$$\begin{aligned} J_{(s,\varepsilon)}(b) &= \int_0^\infty ds\ s^{\varepsilon-1} e^{-bs} \tfrac{1}{2\pi i} \int_{C_w} e^{s\cosh w - |\nu| w} dw \\ &= \tfrac{1}{2\pi i} \int_{C_w} e^{-|\nu| w} dw \int_0^\infty ds\ s^{\varepsilon-1} e^{-\tilde{b}s} \end{aligned} \tag{B.9}$$

where C_w is the contour used in the integral representation of the modified Bessel function (A.10) and parameter $\tilde{b} = b - \cosh w$ is real and positive everywhere on contour C_w. Indeed, $b > 1$ and $\cosh w < 1$ on contour C_w (on horizontal legs $w = \operatorname{Re} w \pm i\pi$ so that $\cosh w = -\cosh(\operatorname{Re} w) < 0$, and on vertical leg $w = i\varphi$, so that $\cosh w = \cos\varphi < 1$). With those provisions made, we integrate over s in (B.9) and manipulate the result as follows:

$$\begin{aligned} \int_0^\infty ds\ s^{\varepsilon-1} e^{-\tilde{b}s} &= \Gamma(\varepsilon) \tilde{b}^{-\varepsilon} \\ &= \Gamma(\varepsilon) \left(1 - \varepsilon \ln \tilde{b} + o(\varepsilon)\right) \\ &= \Gamma(\varepsilon) - \Gamma(1+\varepsilon) \ln \tilde{b} + O(\varepsilon) \\ &= \Gamma(\varepsilon) - \ln \tilde{b} + O(\varepsilon). \end{aligned}$$

The first term, $\Gamma(\varepsilon)$, does not depend on w and is integrated to zero after the last expression is substituted into (B.9), because $\int_{C_w} e^{-|\nu| w} dw = 0$. Dropping $\Gamma(\varepsilon)$ and putting $\varepsilon \to 0$, we get

$$J_{(s)}(b) = -\tfrac{1}{2\pi i} \int_{C_w} \ln(b - \cosh w)\ e^{-|\nu| w} dw = -\frac{1}{|\nu|} \frac{1}{2\pi i} \int_{C_w} e^{-|\nu| w} \frac{\sinh w}{\cosh w - b} dw \tag{B.10}$$

where the last equality is obtained through integration by parts. The integrand is an analytical function of complex variable w and has one single pole at

$$w(b) = \operatorname{arccosh} b = \ln\left(b + \sqrt{b^2 - 1}\right)$$

inside the rectangle surrounded by contour C_w (one side of this rectangle represents vertical interval $(+\infty \pm i\pi)$ located at infinity). Integral (B.10) is readily evaluated with the help of the Cauchy theorem,

$$J_{(s)}(b) = \tfrac{1}{|\nu|} e^{-|\nu| w(b)}. \tag{B.11}$$

Finally, substituting the integral (B.8)

$$J_{(\tau)} = \frac{1}{2|\nu|} \left(\frac{x_K}{x_0}\right)^{-|\nu|/2} \left[e^{-|\nu| w(b)} - e^{-|\nu| w(a)}\right]$$

into the option expression (B.5), and taking into account that $\left(\frac{x_K}{x_0}\right)^{-|\nu|/2} = \sqrt{\frac{F_0}{K}}$, we get a rather simple integral formula for the call option containing only elementary functions

$$C(t,K,F_0) - (F_0-K)^+ = \sqrt{KF_0}\int_0^\infty \frac{dV}{V}\left(\frac{V}{V_0}\right)^{-1/2} \int_{-\infty}^{\infty} \frac{d\xi}{-2\pi i}\sinh\xi\ \frac{e^{-|\nu|w(b)} - e^{-|\nu|w(a)}}{\cosh\xi+\cosh y}\ \frac{e^{-\frac{(\xi+i\pi)^2}{2t}-\frac{t}{8}}}{\sqrt{2\pi t}} \tag{B.12}$$

where

$$\begin{aligned} w(u) &= \operatorname{arccosh} u = \ln(u+\sqrt{u^2-1}) \\ A &= V^2+V_0^2+2VV_0\cosh\xi \\ b &= \tfrac{x_K+x_0}{2\sqrt{x_Kx_0}} > 1 \\ a &= b + \tfrac{A}{2\sqrt{x_Kx_0}} \\ y &= \ln\frac{V}{V_0} \end{aligned}$$

and the denominator in the integrand arises from

$$\tfrac{A}{2VV_0} = \cosh\xi + \tfrac{1}{2}\left(\tfrac{V}{V_0}+\tfrac{V_0}{V}\right) = \cosh\xi+\cosh y. \tag{B.13}$$

B.3 Improving integration with respect to ξ

A direct numerical computation of the option integral (B.12) or Yor's function ϑ (A.11) faces considerable difficulties. Namely, the main exponent imaginary odd part $\operatorname{Im} e^{-\frac{(\xi+i\pi)^2}{2t}} = e^{\frac{\pi^2}{2t}-\frac{\xi^2}{2t}}\sin\frac{\pi\xi}{t}$ contains two problematic factors for implementation. As noted by Carr and Schröder (2004) in a context of Asian options, the factor $e^{\frac{\pi^2}{2t}}$ may be huge, especially for short maturities. This implies that the accompanying integral value containing highly oscillating factor $\sin\frac{\pi\xi}{t}$ is very small and must be computed with extreme accuracy.

For efficient numerical implementation, it is convenient to deform the integration contour to horizontal line $\operatorname{Im}\xi = -\pi$, where $\xi = u - i\pi$ with real u, thus turning complex exponent $e^{-\frac{(\xi+i\pi)^2}{2t}}$ into real Gaussian $e^{-\frac{u^2}{2t}}$.

So far as the Yor function (A.11) is concerned, it is impossible to shift the path of integration far enough down because factor $\exp\{-r\cosh\xi\}$ does not decrease with growing $R = |\operatorname{Re}\xi|$ on far vertical wings $\xi = \pm R - iv$ for $v > \pi/2$. However, the integration with respect to τ, being completed first, changes the behavior of the integrand in (B.12). With $\cosh\xi$ in the denominator, the decaying quadratic exponential $e^{-\frac{(\xi+i\pi)^2}{2t}}$ becomes solely responsible for the

integrand decrease at $|\operatorname{Re}\xi| \to \infty$. Thus, we are allowed to shift the path of integration down, since the integrand can be continued analytically into the whole horizontal strip ($-\pi < \operatorname{Im}\xi < 0$) and falls fast enough at $|\operatorname{Re}\xi| \to \infty$. Placing $\xi = u - i\pi$, with real u , we get

$$C(t,K,F_0) - (F_0-K)^+ = \sqrt{KF_0}\int_0^\infty \frac{dV}{V}\left(\frac{V}{V_0}\right)^{-1/2} \int_{-\infty}^{\infty} \frac{du(-\sinh u)}{-2\pi i}\frac{e^{-|\nu|w(b)} - e^{-|\nu|w(a)}}{-\cosh u + \cosh y}\frac{e^{-\frac{u^2}{2t}-\frac{t}{8}}}{\sqrt{2\pi t}}. \tag{B.14}$$

The denominator turns into zero in two points, $u_{1,2} = \pm y$. However, exactly in these points $A = 0$, so that the numerator in (B.14) also turns into zero. The function as a whole being regular, an integration across these points $u = \pm y$ may be understood in the sense of Cauchy principal value

$$\frac{1}{\cosh u - \cosh y} \to V.P.\frac{1}{\cosh u - \cosh y}.$$

After that, two parts of integral (B.14), associated with terms $e^{-|\nu|w(b)}$ and $e^{-|\nu|w(a)}$, may be considered separately. Since $w(b)$ does not depend on u, the corresponding integral part represents the integral of the odd function and gives zero. As a result, the option time value coincides with the second part

$$\begin{aligned} &C(t,K,F_0) - (F_0-K)^+ \\ &= \sqrt{KF_0}\frac{e^{-\frac{t}{8}}}{\sqrt{2\pi t}}\int_0^\infty dy\ e^{-y/2}\ V.P.\int_{-\infty}^{\infty}\frac{du}{2\pi i}\frac{\sinh u}{\cosh u - \cosh y}\ e^{-|\nu|w(a)-\frac{u^2}{2t}}. \end{aligned}$$

Despite the presence of imaginary unit i in the integral above, it can be shown that the price is real. Indeed, for $\xi = u - i\pi$, the corresponding $\cosh\xi = -\cosh u < 0$. The definition (B.7) suggests that at negative $\cosh\xi$ the real parameter a may be smaller than one or even negative. Since $\cosh w(a) = a$, this means that the exponential

$$e^{-w(a)} = a - \sqrt{a^2-1} = 2\left((a+1)^{1/2} - (a-1)^{1/2}\right)^2$$

may be purely imaginary or complex for different intervals of u. It turns out, however, that the integral as a whole, generates a real value. As follows from the last formula, $e^{-w(a)}$ as a function of u has branch points corresponding to $a = \pm 1$. There are four such points on the real axis u, and a thorough analysis is required to determine correct signs of square roots $(a \pm 1)^{1/2}$ in corresponding intervals. It is too involved (though possible) so we have found a better way to obtain a compact form of the option value.

B.4 Derivation of the alternative expression for option price

The idea is to postpone the integration over w in (B.8) using integral representation (B.10)

$$\begin{aligned} J_{(\tau)} &= \tfrac{1}{2}\left(\frac{x_K}{x_0}\right)^{-|\nu|/2}[J_s(b) - J_s(a)] \\ &= \frac{1}{2|\nu|}\sqrt{\frac{F_0}{K}}\frac{1}{2\pi i}\int_{C_w} dw\, e^{-|\nu|w}\left(\frac{\sinh w}{b-\cosh w} - \frac{\sinh w}{a-\cosh w}\right) \\ &= \frac{1}{2|\nu|}\sqrt{\frac{F_0}{K}}\frac{1}{2\pi i}\int_{C_w} dw\ e^{-|\nu|w}\frac{\sinh w}{[b-\cosh w]\,[a-\cosh w]}\frac{A}{2\sqrt{x_K x_0}} \end{aligned}$$

where, by definition, $a - b = \frac{A}{2\sqrt{x_K x_0}}$. We substitute the last expression into (B.5) and get the option value in the form

$$\begin{aligned} C(t,K,F_0) - (F_0-K)^+ = \sqrt{KF_0}\tfrac{e^{-t/8}}{\sqrt{2\pi t}}\int_{C_w}\tfrac{dw}{2\pi i}\ e^{-|\nu|w}\frac{\sinh w}{b-\cosh w} \\ \int_0^\infty \frac{dV}{V}\left(\frac{V}{V_0}\right)^{-1/2}\frac{VV_0}{\sqrt{x_K x_0}}\int_{-\infty}^{\infty}\tfrac{d\xi}{-2\pi i}\frac{\sinh\xi}{a-\cosh w}e^{-\frac{(\xi+i\pi)^2}{2t}}. \end{aligned} \tag{B.15}$$

Looking for ways to simplify this triple integral with respect to w, V and ξ, we have found that any one of three integrations can be performed explicitly, the other two to be completed numerically. One way is to integrate first over w as we have done in the previous subsection. Another way is to integrate with respect to ξ (again with the help of the residue theory). Then the three legs on contour C_w result in a pure real answer in terms of a double integral over V and w. The third way is to start with integrating over volatility V, which proves to be elementary.

We show the second way starting with integration with respect to the variable ξ. Notice that the denominator $a - \cosh w$ is given by

$$\begin{aligned} a - \cosh w &= \frac{q_K^2 + q_0^2}{2q_K q_0} + \frac{V^2 + V_0^2 + 2VV_0\cosh\xi}{2q_K q_0} - \cosh w \\ &= \frac{VV_0}{q_K q_0}\left(\cosh\xi + \cosh\xi_0(w)\right) \end{aligned} \tag{B.16}$$

where $\cosh\xi_0(w)$ is defined as

$$\cosh\xi_0(w) = \frac{q_K^2 + q_0^2 + V^2 + V_0^2}{2VV_0} - \frac{q_K q_0}{VV_0}\cosh w \tag{B.17}$$

where we switched to an equivalent representation in terms of the Bessel variable $q = x^{1/2}$ rather than the Squared Bessel variable x, i.e.,

$$q_K = \frac{K^{1-\beta}}{1-\beta} \quad \text{and} \quad q_0 = \frac{F_0^{1-\beta}}{1-\beta}. \tag{B.18}$$

Notice that on the contour C_w the hyperbolic cosine $\cosh\xi_0$ as defined by (B.17) takes positive values larger than one. To see it, we rewrite $\cosh\xi_0$ in the form

$$\cosh\xi_0(w) = \frac{V^2+V_0^2}{2VV_0} + \frac{q_Kq_0}{VV_0}\left(\frac{q_K^2+q_0^2}{2q_Kq_0} - \cosh w\right) \geq \frac{V^2+V_0^2}{2VV_0} \geq 1$$

and notice that the second term in the last equality is always positive on the contour C_w. Indeed, on the horizontal legs, $w = \pm i\pi + \mathrm{Re}\, w$ so that $\cosh w = -\cosh(\mathrm{Re}\, w) < 0$ and, on the vertical leg, $w = i\phi$ so that $\cosh w = \cos\phi < 1$ while $\frac{q_K^2+q_0^2}{2q_Kq_0} > 1$. Thus, the function $\xi_0(w)$ takes pure real values on the contour C_w.

Below we will prove that the integration with respect to ξ in (B.15) reduces to

$$J_{(\xi)} = \frac{VV_0}{\sqrt{x_Kx_0}}\int_{-\infty}^{\infty}\frac{d\xi}{-2\pi i}\frac{\sinh\xi}{a-\cosh w}e^{-\frac{(\xi+i\pi)^2}{2t}} \tag{B.19}$$

$$= \int_{-\infty}^{\infty}\frac{d\xi}{-2\pi i}\frac{\sinh\xi}{\cosh\xi+\cosh\xi_0}e^{-\frac{(\xi+i\pi)^2}{2t}} = e^{-\frac{\xi_0^2}{2t}}. \tag{B.20}$$

Indeed, the integrand is an analytical function of ξ on the whole strip $(-2\pi < \mathrm{Im}\,\xi < 0)$ except for two single poles at points $\xi_{1,2} = -i\pi \pm \xi_0$ with equal residues

$$Res\ F(\xi_{1,2}) = \tfrac{1}{-2\pi i}e^{-\frac{\xi_0^2}{2t}}.$$

We close the contour of integration by adding two vertical intervals $|\mathrm{Re}\,\xi| = R \to \infty$ (their contribution is zero) and the horizontal 'return' line $\mathrm{Im}\,\xi = -2\pi$. Making parametrization $\xi = -\xi' - 2\pi i$ (with real ξ') in the return integral shows that it coincides with the original one. Thus, the total integral along the closed contour is a doubled original integral. Finally, the residue Cauchy theorem $2J = -2\pi i\sum_{i=1,2} Res\ F(\xi_i) = 2e^{-\frac{\xi_0^2}{2t}}$ leads to the desired form (B.20).

In the resulting simplified expression for the option value

$$C(t,K,F_0) - (F_0-K)^+ = \sqrt{KF_0}\tfrac{e^{-t/8}}{\sqrt{2\pi t}}\int_0^{\infty}\frac{dV}{V}\left(\frac{V}{V_0}\right)^{-1/2}\int_{C_w}\tfrac{dw}{2\pi i}\,\frac{\sinh w}{b-\cosh w}e^{-|\nu|w}e^{-\frac{\xi_0^2}{2t}} \tag{B.21}$$

concentrate on the complex w-integral along contour the contour C_w. We will reduce it to elementary real integrations suitable for efficient implementation.

The contour C_w consists of three legs. Consider first the vertical leg $w = i\phi$. Since limits of integration are symmetric, $(-\pi < \phi < \pi)$, only the even part of the integrand as a whole contributes to the answer, resulting in the following w-integral along the vertical line

$$\frac{1}{\pi}\int_0^{\pi} d\phi\frac{\sin\phi\ \sin(|\nu|\phi)}{b-\cos\phi}e^{-\frac{\xi_0^2}{2t}}.$$

Next, on the two horizontal legs, we parameterize $w = \pm i\pi + \psi$ with real positive ψ. Integrands for the upper and lower legs differ only by factors $e^{\mp i|\nu|\pi}$. As a result, the contribution to the w-integral from two horizontal legs of the contour C_w reads as

$$\frac{\sin(|\nu|\pi)}{\pi}\int_0^\infty d\psi \frac{\sin\psi}{b+\cosh\psi} e^{-|\nu|\psi} e^{-\frac{\xi_0^2}{2t}}.$$

Summarizing, we come up with the following expression for the option value

$$\begin{aligned} C(t,K,F_0) - (F_0-K)^+ &= \sqrt{KF_0}\frac{e^{-t/8}}{\sqrt{2\pi t}}\int_0^\infty \frac{dV}{V}\left(\frac{V}{V_0}\right)^{-1/2} \\ &\left\{\frac{1}{\pi}\int_0^\pi d\phi \frac{\sin\phi\ \sin(|\nu|\phi)}{b-\cos\phi} e^{-\frac{\xi_0(w,V)^2}{2t}} + \frac{\sin(|\nu|\pi)}{\pi}\int_0^\infty d\psi \frac{\sinh\psi}{b+\cosh\psi} e^{-|\nu|\psi} e^{-\frac{\xi_0(w,V)^2}{2t}}\right\} \end{aligned} \tag{B.22}$$

where

$$\begin{aligned} b &= \frac{q_K^2+q_0^2}{2q_Kq_0} \\ \xi_0(w,V) &= \operatorname{arccosh}\left\{\frac{q_K^2+q_0^2+V^2+V_0^2}{2VV_0} - \frac{q_Kq_0}{VV_0}\cosh w\right\} \end{aligned} \tag{B.23}$$

and

$$\begin{aligned} \cosh w = \cosh i\phi = \cos\phi \qquad &\text{for } \phi\text{-integral,} \\ \cosh w = \cosh(\pm i\pi + \psi) = -\cosh\psi \quad &\text{for } \psi\text{-integral.} \end{aligned}$$

One can find appearance similarities of the option price (B.22) with the Heat-Kernel in polar coordinates on the two-dimensional plane, see Lipton-Sepp (2011).

B.5 Another form of solution

In this subsection, we will recast the expression (B.22) into a more compact form.

In the double integral (B.22), change the order of integration, starting with V

$$J_{(V)} = \frac{e^{-t/8}}{\sqrt{2\pi t}}\int_0^\infty \frac{dV}{V}\left(\frac{V}{V_0}\right)^{-1/2} e^{-\frac{\xi_0(w,V)^2}{2t}}.$$

Denoting

$$D(w)^2 = \frac{q_K^2+q_0^2-2q_Kq_0\cosh w + V_0^2}{V_0^2}, \tag{B.24}$$

we can rewrite $\cosh\xi_0$ (B.23) as

$$\cosh\xi_0(w,V) = D\left(\frac{DV_0}{2V} + \frac{V}{2DV_0}\right) = D(w)\cosh\bar{y} \tag{B.25}$$

with parametrization

$$\frac{V}{DV_0} = e^{\bar{y}}.$$

Note that this parametrization differs from the usual one, $\frac{V}{V_0} = e^{y}$. Accepting $\bar{y}$ as an integration variable, we recast the V-integral into

$$J_{(V)} = \tfrac{e^{-t/8}}{\sqrt{2\pi t}}\, D^{-1/2} \int_{-\infty}^{\infty} d\bar{y}\; e^{-\frac{\bar{y}}{2}} e^{-\frac{{\xi_0}^2}{2t}} = 4\, \tfrac{e^{-t/8}}{\sqrt{2\pi t}}\, D^{-1/2} \int_{0}^{\infty} d(\sinh\tfrac{\bar{y}}{2}) e^{-\frac{{\xi_0}^2}{2t}}.$$

Now taking ξ_0 itself as an integration variable, $u = \xi_0$, expressing $\sinh\frac{\bar{y}}{2}$ through u using (B.25),

$$\sinh\tfrac{\bar{y}}{2} = \sqrt{\frac{\cosh\bar{y} - 1}{2}} = \sqrt{\frac{\cosh u - D}{2D}}$$

and denoting $D = \cosh s$ for $s > 0$, we can further simplify the integral

$$\begin{aligned} J_{(V)} &= \tfrac{e^{-t/8}}{\sqrt{2\pi t}} \int_0^{\infty} \frac{dV}{V} \left(\frac{V}{V_0}\right)^{-1/2} e^{-\frac{\xi_0(w,V)^2}{2t}} \\ &= \frac{2\sqrt{2}}{\cosh s} \frac{e^{-t/8}}{\sqrt{2\pi t}} \int_s^{\infty} d(\sqrt{\cosh u - \cosh s}) e^{-\frac{u^2}{2t}} = \frac{1}{\cosh s} G(t,s). \end{aligned} \tag{B.26}$$

The function $G(t,s)$ can be represented in various forms

$$G(t,s) = 2\sqrt{2}\frac{e^{-t/8}}{\sqrt{2\pi t}} \int_s^{\infty} d(\sqrt{\cosh u - \cosh s}) e^{-\frac{u^2}{2t}} \tag{B.27}$$

$$\begin{aligned} &= \sqrt{2}\frac{e^{-t/8}}{\sqrt{2\pi t}} \int_s^{\infty} du \frac{\sinh u}{\sqrt{\cosh u - \cosh s}} e^{-\frac{u^2}{2t}} \\ &= 2\sqrt{2}\frac{e^{-t/8}}{t\sqrt{2\pi t}} \int_s^{\infty} du \sqrt{\cosh u - \cosh s}\;\; u\, e^{-\frac{u^2}{2t}}. \end{aligned} \tag{B.28}$$

The last form is convenient for numerical computation. It is worth noticing also that the derivative of function G is equal to

$$-\frac{1}{\sinh s}\frac{\partial G}{\partial s} = \sqrt{2}\frac{e^{-t/8}}{t\sqrt{2\pi t}} \int_s^{\infty} \frac{du\, u\, e^{-\frac{u^2}{2t}}}{\sqrt{\cosh u - \cosh s}} = 2\pi G^{(2)}(t,s)$$

where $G^{(2)}(t,s)$ is exactly the McKean heat kernel for the H^2 Poincare hyperbolic plane.

Using expression (B.26) for the V-integral, we get the following option value (B.22)

$$\begin{aligned} C(t,K,F_0) - (F_0 - K)^+ = \frac{1}{\pi}\sqrt{KF_0} \Bigg\{ &\int_0^{\pi} d\phi \frac{\sin\phi\;\; \sin(|\nu|\phi)}{b - \cos\phi} \frac{G(t,s)}{\cosh s} \\ &+ \sin(|\nu|\pi) \int_0^{\infty} d\psi \frac{\sinh\psi}{b + \cosh\psi} e^{-|\nu|\psi} \frac{G(t,s)}{\cosh s} \Bigg\}. \end{aligned} \tag{B.29}$$

It may be convenient to pass to s as a integration variable. From the definition $\cosh s = D$, it follows that

$$\cosh^2 s = D^2 = \frac{q_K^2 + q_0^2 - 2q_K q_0 \cosh w}{V_0^2} + 1$$

and

$$\sinh^2 s = \frac{q_K^2 + q_0^2 - 2q_K q_0 \cosh w}{V_0^2} = \frac{2q_K q_0}{V_0^2}(b - \cosh w). \tag{B.30}$$

Consider the simplified option expression (B.29) where $\cosh w = \cos\phi$ in the first integral and $\cosh w = -\cosh\psi$ in the second one. Limits of integration over s are $\{s_- < s < s_+\}$ for ϕ-integral and $\{s_+ < s\}$ for ψ-integral. Here $s_- > 0$ is defined at $\phi = 0$ ($w = 0$) and $s_+ > 0$ is defined at $\phi = \pi$, or $\psi = 0$ ($w = i\pi$),

$$\sinh^2 s_- = \frac{2q_K q_0}{V_0^2}(b-1) = \frac{(q_K - q_0)^2}{V_0^2} \tag{B.31}$$

$$\sinh^2 s_+ = \frac{2q_K q_0}{V_0^2}(b+1) = \frac{(q_K + q_0)^2}{V_0^2}. \tag{B.32}$$

Differentials and functions involved are expressed through s as follows

$$\begin{aligned}\frac{1}{\cosh s} d\phi \frac{\sin\phi}{b - \cos\phi} &= \frac{1}{\cosh s} d\left[\ln(b - \cos\phi)\right] \\ &= \frac{1}{\cosh s} d\left[\ln \sinh^2 s\right] \\ &= 2\frac{ds}{\sinh s}.\end{aligned}$$

The same is valid for ψ

$$\frac{1}{\cosh s} d\psi \frac{\sinh\psi}{b + \cosh\psi} = 2\frac{ds}{\sinh s}.$$

Now, we express ϕ and ψ through the integration parameter s using the above definitions (B.30, B.31, B.32)

$$\tan^2\frac{\phi}{2} = \frac{1 - \cos\phi}{1 + \cos\phi} = \frac{\sinh^2 s - \sinh^2 s_-}{\sinh^2 s_+ - \sinh^2 s} \tag{B.33}$$

$$\tanh^2\frac{\psi}{2} = \frac{\cosh\psi - 1}{\cosh\psi + 1} = \frac{\sinh^2 s - \sinh^2 s_+}{\sinh^2 s - \sinh^2 s_-}. \tag{B.34}$$

Finally, the call option value reads as

$$C(t,K,F_0) - (F_0 - K)^+ = \\ \frac{2}{\pi}\sqrt{KF_0}\left\{\int_{s_-}^{s_+} ds \frac{\sin(|\nu|\phi(s))}{\sinh s} G(t,s) + \sin(|\nu|\pi)\int_{s_+}^{\infty} ds \frac{e^{-|\nu|\psi(s)}}{\sinh s} G(t,s)\right\} \tag{B.35}$$

with the explicitly defined underlying functions

$$\phi(s) = 2\,\arctan\sqrt{\frac{\sinh^2 s - \sinh^2 s_-}{\sinh^2 s_+ - \sinh^2 s}} \tag{B.36}$$

$$\psi(s) = 2\,\mathrm{arctanh}\sqrt{\frac{\sinh^2 s - \sinh^2 s_+}{\sinh^2 s - \sinh^2 s_-}} \tag{B.37}$$

the integration limits

$$s_- = \mathrm{arcsinh}\left(\frac{|q_K - q_0|}{V_0}\right) \tag{B.38}$$

$$s_+ = \mathrm{arcsinh}\left(\frac{q_K + q_0}{V_0}\right) \tag{B.39}$$

and the Kernel function $G(t,s)$ given by (B.27).

C Effective zero correlation SABR: ATM parameters

In this section, we take an ATM limit for the effective volatility (6.38) and its correction (6.44). This corresponds to a case when the strike $K = F_0 + \delta K$ approaches the forward value $K \to F_0$ and naturally implies that $\delta q \to 0$ and $\delta\tilde{q} \to 0$ where as usual

$$\delta q = \frac{K^{1-\beta} - F_0^{1-\beta}}{1-\beta} \quad \text{and} \quad \delta\tilde{q} = \frac{K^{1-\tilde{\beta}} - F_0^{1-\tilde{\beta}}}{1-\tilde{\beta}}. \tag{C.1}$$

Adopting notations $\delta z = \gamma\frac{\delta q}{v_0}$, we calculate small δz expansion of the following

$$\begin{aligned}
v_{\min} &= \sqrt{\gamma^2\delta q^2 + 2\rho\gamma\delta q v_0 + v_0^2} = v_0\left(1 + \rho\,\delta z + \frac{1}{2}(1-\rho^2)\,\delta z^2 - \frac{1}{2}\rho\,(1-\rho^2)\,\delta z^3 + O(\delta z^4)\right)\\
\phi &= \frac{v_{\min} + \rho v_0 + \gamma\delta q}{(1+\rho)v_0} = 1 + \delta z + \frac{1}{2}(1-\rho)\,\delta z^2 - \frac{1}{2}\rho\,(1-\rho)\,\delta z^3 + O(\delta z^4)\\
\Phi &= \phi^{\frac{\tilde{\gamma}}{\gamma}} = 1 + a\delta z + \frac{1}{2}a(a-\rho)\,\delta z^2 + \frac{1}{6}\,a\,\left(3\rho^2 - 1 - 3a\rho + a^2\right)\delta z^3 + O(\delta z^4)
\end{aligned}$$

where $a = \frac{\tilde{\gamma}}{\gamma}$. This gives the first terms of the Taylor expansion in small δq of the effective volatility (6.38)

$$\tilde{v}_0^{(0)} = \frac{2\,\Phi\,\delta\tilde{q}\,\tilde{\gamma}}{\Phi^2 - 1} = v_0\frac{\delta\tilde{q}}{\delta q}\left(1 + \frac{1}{2}\rho\,\gamma\frac{\delta q}{v_0} + \frac{1}{6}\,\left(1 - \frac{\tilde{\gamma}^2}{\gamma^2} - \frac{3}{2}\rho^2\right)\gamma^2\frac{\delta q^2}{v_0^2} + O(\delta q^3)\right), \tag{C.2}$$

leading to the desired limits (2.33) and (2.35).

The volatility correction (6.44) ATM limit is more complicated because the first non-vanishing order of both numerator and denominator is of $O(\delta K^2)$. We first concentrate on the parallel transport expansion (6.12), where the integral $\mathcal{B}_{\min}$ in (6.17) has the second order in δK. The angle $\varphi_0+\alpha$ is close to π, thus we can expand the denominator in the integrand for small $\sin\varphi'$ to obtain

$$\mathcal{B}_{\min} \simeq -\frac{1}{2}\frac{\beta}{1-\beta}\cot\alpha\, L\int_{\varphi_0+\alpha}^{\pi}\sin\varphi'\,d\varphi' = \frac{1}{2}\frac{\beta}{1-\beta}\cot\alpha\, L\left(\cos\pi-\cos(\varphi_0+\alpha)\right).$$

Taking into account

$$\sin(\varphi_0+\alpha) = -\frac{\delta q}{R} = -\frac{\delta q\gamma\sin\alpha}{v_{\min}} = -\frac{\delta q\gamma\sin\alpha}{v_0}\left(1+O(\delta q)\right),$$

we obtain

$$\mathcal{B}_{\min} = -\frac{1}{4}\frac{\beta}{1-\beta}\rho\,\frac{\delta q^2\,\gamma}{q_0 v_0}+O(\delta q^3)$$

where we have used the leading value $L\simeq\frac{V_0}{q_0\,\sin\alpha}$. Thus, the parallel transport expands as follows

$$\mathcal{A}_{\min} = \frac{1}{2}\beta\ln(K/F_0)+\mathcal{B}_{\min} = \frac{1}{2}\beta\ln(1+\delta K/F_0)-\frac{1}{4}\frac{\beta}{1-\beta}\rho\,\frac{\delta q^2\,\gamma}{q_0 v_0}+O(\delta q^3). \tag{C.3}$$

Note that the zero correlation of the parallel transport is simply potential

$$\tilde{\mathcal{A}}_{\min} = \frac{1}{2}\tilde{\beta}\ln(1+\delta K/F_0).$$

Now we expand the expression $\ln\left(\sqrt{v_0 v_{\min}}\right)$ and $\ln\left(\tilde{v}_0^{(0)}\,\tilde{v}_{\min}^{(0)}\right)$ up to the second order in the volatility correction (6.44)

$$\begin{aligned}
\ln\left(v_0 v_{\min}\right) &= 2\ln v_0+\rho\,\gamma\frac{\delta q}{v_0}+\frac{1}{2}(1-2\rho^2)\,\gamma^2\frac{\delta q^2}{v_0^2}+O(\delta q^3)\\
\ln\left(\tilde{v}_0^{(0)}\,\tilde{v}_{\min}^{(0)}\right) &= 2\ln\tilde{v}_0^{(0)}+\frac{1}{2}\,\tilde{\gamma}^2\frac{\delta\tilde{q}^2}{\left(\tilde{v}_0^{(0)}\right)^2}+O(\delta q^3).
\end{aligned}$$

Consider a *special case* of $\beta=\tilde{\beta}$ resulting in $\delta q=\delta\tilde{q}$. Then, the main order ATM volatility $\tilde{v}_0^{(0)}$ expansion reads

$$\tilde{v}_0^{(0)} = v_0\left(1+\frac{1}{2}\rho\,\gamma\frac{\delta q}{v_0}+\frac{1}{6}\left(1-\frac{\tilde{\gamma}^2}{\gamma^2}-\frac{3}{2}\rho^2\right)\gamma^2\frac{\delta q^2}{v_0^2}+O(\delta q^3)\right). \tag{C.4}$$

This leads to the desired ATM value

$$\tilde{v}_0^{(0)}\Big|_{K=F_0} = v_0. \tag{C.5}$$

Next, we have

$$\ln\left(\tilde{v}_0\,\tilde{v}_{\min}\right) \;=\; 2\ln v_0 + \rho\,\gamma\frac{\delta q}{v_0} + \frac{1}{3}\left(1 + \frac{1}{2}\frac{\tilde{\gamma}^2}{\gamma^2} - \frac{9}{4}\rho^2\right)\gamma^2\frac{\delta q^2}{v_0^2} + O(\delta q^3)$$

and

$$\ln\left(v_0 v_{\min}\right) - \ln\left(\tilde{v}_0\,\tilde{v}_{\min}\right) \;=\; \frac{1}{6}\left(1 - \frac{\tilde{\gamma}^2}{\gamma^2} - \frac{3}{2}\rho^2\right)\gamma^2\frac{\delta q^2}{v_0^2} + O(\delta q^3).$$

Then, we obtain the numerator (6.44) expansion

$$\begin{aligned} & \ln\left(K^{\beta}\sqrt{v_0 v_{\min}}\right) - \ln\left(K^{\tilde{\beta}}\sqrt{\tilde{v}_0\tilde{v}_{\min}}\right) + \tilde{\mathcal{A}}_{\min} - \mathcal{A}_{\min} \\ = \;& \frac{1}{12}\left(1 - \frac{\tilde{\gamma}^2}{\gamma^2} - \frac{3}{2}\rho^2\right)\gamma^2\frac{\delta q^2}{v_0^2} + \frac{1}{4}\frac{\beta}{1-\beta}\rho\,\frac{\delta q^2\,\gamma}{q_0 v_0} + O(\delta q^3) \end{aligned}$$

and this of the denominator

$$\Omega = \frac{\delta q^2\tilde{\gamma}^2}{v_0^2} + O(\delta q^3).$$

This leads to the desired result of the ATM value of the effective volatility correction (2.34) for $\beta = \tilde{\beta}$

$$\left.\frac{\tilde{v}_0^{(1)}}{\tilde{v}_0^{(0)}}\right|_{K=F_0} \;=\; \frac{1}{12}\left(1 - \frac{\tilde{\gamma}^2}{\gamma^2} - \frac{3}{2}\rho^2\right)\gamma^2 + \frac{1}{4}\frac{\beta}{1-\beta}\rho\,\frac{v_0\gamma}{q_0} \tag{C.6}$$

$$\;=\; \frac{1}{12}\left(1 - \frac{\tilde{\gamma}^2}{\gamma^2} - \frac{3}{2}\rho^2\right)\gamma^2 + \frac{1}{4}\,\beta\,\rho\;\, v_0\gamma\, F_0^{\beta-1}. \tag{C.7}$$

The general case $\beta \neq \tilde{\beta}$ correction (2.36) derivation can be done similarly.